The Pharmacokinetics, Metabolism, and Clearance Mechanisms of Abrocitinib, a Selective Janus Kinase Inhibitor, in Humans

Jonathan N. Bauman, Angela C. Doran, Amanda King-Ahmad, Raman Sharma, Gregory S. Walker, Jian Lin, Tsung H. Lin, Jean-Baptiste Telliez, Sakambari Tripathy, Theunis C. Goosen, Christopher Banfield, Bimal K. Malhotra, and Martin E. Dowty

Medicine Design, Pfizer Inc., Cambridge, MA (M.E.D) and Groton, CT (J.N.B., A.C.D., A.K-A., R.S., G.S.W., J.L., T.C.G.); Inflammation and Immunology, Pfizer Inc., Cambridge, MA (T.H.L., J-B.T.); Clinical Pharmacology, Pfizer Inc., Cambridge, MA (C.B.), Groton, CT (S.T.), and New York, NY (B.K.M.)

Running title: Human ADME properties of abrocitinib

Address correspondence to:

Martin E. Dowty

Pfizer Inc.

1 Portland St

Cambridge, MA 02139

Email: martin.dowty@pfizer.com

Phone: (617) 981-9722

Text pages: 40

Tables: 8

Figures: 5

References: 11

Number of words in Abstract: 196

Number of words in Introduction: 601

Number of words in Discussion: 604

Abbreviations: ADME, absorption, distribution, metabolism, excretion; AMS, accelerator mass spectroscopy; AUC, area under the curve; AUC_{inf}, area under the concentration-time curve from time 0 to infinity; B/P, blood to plasma ratio; CL, clearance; CL_b, blood clearance; CL_{int}, intrinsic clearance; $CL_{int,app}$, apparent intrinsic clearance; $CL_{int,app\ sc}$, scaled in vivo apparent intrinsic clearance; CL_r, renal clearance; C_{max}, maximum concentration; COSY, homonuclear correlation spectroscopy; CYP, cytochrome P450; DMSO, dimethylsulfoxide; EM, extensive metabolizer; F, bioavailability; $f_a f_g$, fraction absorbed × fraction surviving gut metabolism; f_{CL}, fraction of clearance; f_m, fraction of metabolism; $f_{mMx,CYPz}$, fraction metabolism represented by a single metabolite x and specific CYP isoform z; f_u, fraction unbound in plasma; HLM, human liver microsome; HMBC, heteronuclear multiple bond correlation spectroscopy; HPLC, high performance liquid chromatography; hWB, human whole blood; IC_{50}, half maximal inhibition concentration; IFN, interferon; IL, interleukin; IV, intravenous; JAK, Janus kinase; Km, apparent substrate concentration at half-maximal velocity; Ki, inhibition constant for substrates exhibiting substrate inhibition kinetics; LC-MS, liquid chromatography-mass spectrometry; LC-MS/MS, liquid chromatography-tandem mass spectrometry; MRM, multiple reaction monitoring; MSn, tandem mass spectrometry scans; NADPH, nicotinamide adenine dinucleotide phosphate; PPP, 2-phenyl-2-(1-piperdinyl)propane; QC, quality control; RM, rapid metabolizer; S, substrate concentration; S_{50}, substrate concentration at half-maximal velocity; STAT, signal transducer and activator of transcription; $t_{1/2}$, half-life; T_{max}, time to maximum plasma concentration; TYK, tyrosine kinase; UHPLC, ultra-high-performance liquid chromatography; V, rate of product formation; V_{max}, maximum rate of metabolism; V_{ss}, steady state volume of distribution

Abstract

Abrocitinib is an oral once-daily Janus kinase 1 selective inhibitor being developed for the treatment of moderate-to-severe atopic dermatitis. This study examined the disposition of abrocitinib in male participants following oral and intravenous administration using accelerator mass spectroscopy methodology to estimate pharmacokinetic parameters and characterize metabolite profiles. The results indicated abrocitinib had a systemic clearance of 64.2 L/h, a steady state volume of distribution of 100 L, extent of absorption >90%, time to maximum plasma concentration of ~0.5 hour, and absolute oral bioavailability of 60%. The half-life of both abrocitinib and total radioactivity was similar with no indication of metabolite accumulation. Abrocitinib was the main circulating drug species in plasma (~26%) with 3 major mono-hydroxylated metabolites (M1, M2, and M4) at >10%. Oxidative metabolism was the primary route of elimination for abrocitinib with the greatest disposition of radioactivity shown in the urine (~85%). In vitro phenotyping indicated abrocitinib cytochrome P450 fraction of metabolism assignments of 0.53 for CYP2C19, 0.30 for CYP2C9, 0.11 for CYP3A4, and ~0.06 for CYP2B6. The principal systemic metabolites M1, M2, and M4 were primarily cleared renally. Abrocitinib, M1, and M2 showed pharmacology with similar Janus kinase 1 selectivity, whereas M4 was inactive.

Significance statement

This study provides a detailed understanding of the disposition and metabolism of abrocitinib, a JAK inhibitor for atopic dermatitis, in humans, as well as characterization of clearance pathways and pharmacokinetics of abrocitinib and its metabolites.

5

Introduction

Abrocitinib (PF-04965842) is a selective small molecule Janus kinase 1 (JAK1) inhibitor under development at daily doses of 200 and 100 mg to treat moderate-to-severe atopic dermatitis (Gooderham et al., 2019; Silverberg et al., 2020; Simpson et al., 2020; Bieber et al., 2021). Selective inhibition of cytokines by abrocitinib that signal through JAK1 dependent pairs (i.e., JAK1/JAK2, JAK1/JAK3, and JAK1/tyrosine kinase [TYK] 2) includes interleukin (IL)-4, IL-13, and other cytokines (e.g., IL-31, IL-22, and thymic stromal lymphopoietin) involved in the pathogenesis of atopic dermatitis and pruritus (Trier and Kim, 2018) while sparing non-JAK1 pairs such as JAK2/JAK2 inhibition and thereby minimizing the risk for neutropenia and anemia (Akada et al., 2014).

Abrocitinib is a weak base of molecular weight 323.4 with measured logP of 1.7 and pK_a of 5.2 (data on file). Abrocitinib showed high in vitro permeability in Madin-Darby Canine Kidney cells at 16×10^{-6} cm/s. Aqueous solubility was pH dependent at ~8 mg/mL at pH ~1 and ~35 μg/mL at pH ~8. Abrocitinib pharmacokinetics have been investigated in healthy volunteers (Peeva et al., 2018). Abrocitinib was absorbed rapidly following single doses of 3 to 200 mg (the median time that maximum plasma concentration [C_{max}] occurred [T_{max}] was <1 hour) and more slowly at higher doses of 400 and 800 mg (median T_{max} 1.5-4.0 hours), indicating some delayed absorption at higher doses. Plasma C_{max} increased proportionally from 3 to 800 mg; the area under concentration-time curve extrapolated to infinity (AUC_{inf}) was greater than proportional with doses of 400 and 800 mg. Multiple dose pharmacokinetics showed steady state was reached by day 4 with an observed accumulation ratio of 1.3 to 1.5 with once-daily dosing between 30 and 200 mg and plasma half-life ranged between approximately 2 and 4 hours. Renal clearance of abrocitinib was estimated to between 0.59 to 0.67 L/h (Peeva et al., 2018).

6

Examining human radiolabeled absorption, distribution, metabolism, and excretion (ADME) provides a comprehensive profile of the disposition of a drug. Recent application of accelerator mass spectrometry (AMS) analytical methodology to human ADME studies has been an important advancement in study design, as this enables administration of up to 1000-fold lower doses of carbon-14 compared to traditional methods of study (Spracklin et al., 2020). Using microtracer of carbon-14 (0.1-1 μCi) administration, more informative ADME studies that include two-period fixed sequence oral (Period A) and intravenous (IV) (Period B) designs can be performed; these studies allow the determination of additional drug parameters including systemic clearance, volume of distribution, gut availability, and absolute bioavailability. In addition, the low level of radioactivity eliminates the need for the prerequisite quantitative whole-body autoradiography rat study to estimate dosimetry or the need to run nonclinical safety studies with an IV formulation, since the microtracer is adequately supported by oral toxicology studies. An important design element of the microtracer IV period is the administration of a clinically relevant non-labeled dose of the drug, followed by the administration of the IV microtracer of ^{14}C-drug at approximately T_{max} in order to reflect an appropriate total mass of drug in the body and allow scaling of the IV pharmacokinetic parameters to a therapeutic dose (Spracklin et al., 2020).

The objectives of the present fixed-dose cross-over oral and IV study were to investigate the disposition, mass balance, and metabolic profiles of a therapeutic oral dose of 200 mg abrocitinib in healthy participants as well as determine its systemic clearance, volume of distribution, gut availability, and absolute bioavailability. In addition, metabolic clearance mechanisms of abrocitinib were investigated with in vitro hepatic systems and in vitro

pharmacology of both abrocitinib and primary circulating metabolites was assessed in human

whole cell assays.

Materials and Methods

Materials and Reagents. Abrocitinib (PF-04965842), its deuterated standard (PF-06651703), and metabolites M1 (PF-06471658), M2 (PF-07055087), M3 (PF-07055090), M4 (PF-07054874), M5 (PF-07054926), M6 (PF-07095462), M7 (PF-06737821), and 2-phenyl-2-(1-piperdinyl) propane (PPP), were synthesized at Pfizer Inc (Groton, CT). ^{14}C-abrocitinib (^{14}C label on the 2-position of the carbon of the pyrimidine ring) was synthesized by Perkin Elmer Inc (Boston, MA), with radiochemical purity of 98.3% and specific radioactivity of 6.31 µCi/mg. Analytical chemicals of analytical grade or better were obtained from Fischer Scientific (Waltham, MA). MgCl$_2$, β-nicotinamide adenine dinucleotide 2´-phosphate reduced tetrasodium salt (NADPH), diclofenac, furafylline, tienilic acid, esomeprazole, quinidine, aminobenzotriazole, 1 M potassium phosphate dibasic solution, 1 M potassium phosphate monobasic solution, sodium bicarbonate, and dimethylsulfoxide (DMSO) were purchased from Sigma Aldrich (St. Louis, MO). Troleandomycin was ordered from Fischer Scientific (Waltham, MA), and gemfibrozil acyl glucuronide was synthesized at Wuxi App Tec (Shanghai, China). HPLC solvents included ammonium acetate, acetonitrile, methanol, and formic acid from Biosolve (Valkenswaard, Netherlands); trifluoracetic acid from Sigma Aldrich (Amsterdam, Netherlands); isopropyl amine from iPAm, Merck (Amsterdam, Netherlands); 2mM ammonium acetate/methanol/acetonitrile (95/2.5/2.5 % v/v) from Brand-Nu Laboratories (Meriden, CT); and methanol, acetonitrile, and water from J.T. Baker (Avantor, Radnor, PA). Cell culture medium included Williams E media (GIBCO-BRL custom formula Lot# 1701813) and HEPES (Lonza, Switzerland). Pooled human liver microsomes (HLM) (HLM103, 20.0 mg protein/ml, 0.31 nmol CYP/mg protein) were prepared and characterized by Sekisui Xenotech (Kansas City, KS) from 50 individual human donors of both sexes. Cryopreserved human hepatocytes (lot DCM) were

9

prepared and characterized by Bioreclamation IVT (Baltimore, MD) from 10 individual donors of both sexes.

Clinical Study and Sample Collection. This study was a phase I, open-label, non-randomized, 2-period, fixed sequence study conducted at PRA-EDS International (Groningen, Netherlands). Six healthy male participants (1 Hispanic/5 Non-Hispanic), 22-28 years of age, with a mean body weight of 83.1 kg and body mass index of 24.4 kg/m^2 were enrolled. Participants were genotyped for CYP2C19 and 2C9 with commercially available TaqMan assays and analyzed on a QuantStudio 12K Flex Real-Time PCR System. Each participant received 2 dose regimens in periods A and B (14 days following Period A) following an overnight fast. Period A was an oral solution dose of 200 mg abrocitinib and 80 μg ^{14}C-abrocitinib. Plasma samples were collected before dosing and from 0.25 to 96 hours after dose. Urine and feces were collected prior to dose and up to 240 hours following dose (excreta collection continued until at least 90% of administered dose was recovered or less than 1% was recovered from excreta from 2 consecutive days). Period A samples were analyzed for total ^{14}C and metabolite profiling. Period B was an oral solution dose of 200 mg abrocitinib followed by a 100 μg ^{14}C-abrocitinib IV approximately 1 hour later (T_{max}). Plasma samples were collected before dose and at various times after post and analyzed for total ^{14}C, ^{14}C-abrocitinib (0.083 to 95 hours post-IV dose), and abrocitinib (0.25 to 96 hours following oral dose) concentrations. Urine was collected before dose and up to 143 hours post-IV dose and analyzed for total ^{14}C radioactivity. Feces were not collected in Period B based on the observation that <10% of dose was recovered in feces in Period A. The final protocol and informed consent documentation were reviewed and approved by the Independent Ethics Committee at the investigational center participating in the study. This study was conducted in compliance with the ethical principles originating in or derived from the

Declaration of Helsinki and in compliance with all International Council for Harmonization

Good Clinical Practice Guidelines.

Radiochemical Analysis. Analyses of total ^{14}C radioactivity in plasma, urine, and feces

homogenate were conducted at TNO (Microbiology and Systems Biology, Zeist, Netherlands)

using ^{14}C detection by AMS. AMS analysis was performed on a 1MV multi-element AMS,

model 4110 Bo, High Voltage Engineering (software: AMS 155). Low-level scintillation

counting was performed on a Quantulus 1220 (software WinQ version 1.2). Aliquots of plasma

(5 µL), urine (15 µL, diluted or undiluted) or feces homogenate (homogenized at the PRA Health

Sciences Bioanalytical Laboratory (Drenthe, Netherlands), 30 mg, diluted or undiluted,) was

transferred to tinfoil cups. The samples were dried under a stream of nitrogen and subsequently

placed in the elemental analyzer (Vario Micro; Elementar, Langenselbold, Germany) which

acted as autosampler and CO_2 combustion device for the AMS (van Duijn et al, 2014). The

natural background $^{14}C/^{12}C$ level, measured in predose samples of each matrix, was subtracted to

obtain the amount of ^{14}C abrocitinib-related ^{14}C. $^{14}C/^{12}C$ isotope ratios of the samples were

converted to mBq/mL for plasma and urine samples, whereas the homogenized feces samples

data were converted into mBq/g. The total ^{14}C radioactivity concentrations in urine and feces

were further converted to percentage of dose recovered in urine and feces based upon the

radioactivity dose administered to each participant. A reference standard ANU sucrose-8542

with a certificated $^{14}C/^{12}C$ isotope ratio was used as system suitability sample. In each batch, the

measured $^{14}C/^{12}C$ ratio deviated <15% from the certified ratio. Plasma standard samples were

included in each analysis as AMS quality control (QC) samples with a minimum of 3 replicates.

The samples were prepared by spiking blank pooled plasma with a known amount of ^{14}C (from

[14]C-paracetamol). The ^{14}C/^{12}C ratios were determined by AMS and found to deviate no more than 15% from the nominal value. In addition, the CV was also <15%.

Metabolite Profiling in Plasma, Urine, and Feces

Sample Preparation. To profile circulating metabolites, plasma samples from each individual at 0-12 hours post-dose, which covered >97% of the total radioactivity area under-the-curve (AUC), were pooled according to the method of Hamilton et al. (Hamilton et al., 1981). The pre- and postdose pools were prepared using equal volumes from each participant. The pooled plasma (100 µL) was diluted with acetonitrile (500 µL), vortexed for 1 minute and centrifuged (14,000g, 5 minutes, 10°C). After centrifugation, 500 µL supernatant was removed and dried under a stream of nitrogen. The residue was dissolved in 2 mM ammonium acetate:acetonitirile:methanol (80:10:10 % v:v:v) and vortexed for 30 seconds, and centrifuged (1000g, 1 minute, room temperature). Urine samples collected from each participant from 0 to 12 hours following dosing represented 96% of the excreted radioactivity. A pre-dose pool was prepared by mixing equal volumes of each pre-dose sample. An equal volume from each individual was pooled, 50 µL of urine sample, 700 µL 2 mM ammonium acetate:acetonitirile:methanol (80:10:10 % v:v:v) was added, vortexed for 1 minute, and centrifuged (1000g, 1 minute, room temperature). Individual fecal homogenate pools accounting for 97% of the total dose collected from feces were prepared for each participant by combining proportional amounts of the sample collected over each time period (48-144 hours, 24-96 hours, 24-72 hours, 48-168 hours, 0-48 hours, 0-72 hours, respectively). An equal amount from each individual participant pool was then combined into a master pool. A pooled pre-dose sample was prepared by taking equal aliquots per participant. To a 100 mg of feces homogenate sample, 500 µL acetonitrile was added, equilibrated for 5 minutes, and vortexed for 1 minute. The sample

12

was centrifuged (14,000g, 5 minutes, 10 °C) and 500 μL supernatant was removed and a second extraction was performed using the same methods. The residue was dissolved in 2 mM ammonium acetate:acetonitirile:methanol (80:10:10 % v:v:v), vortexed for 30 seconds, and centrifuged (1000g, 1 minute, room temperature). Sample extraction and liquid chromatography-mass spectrometry (LC-MS) profiling column recoveries were all greater than 89%.

Metabolite Profiling Ultra-High-Performance Liquid Chromatography (UHPLC) Methods. Pooled urine and extracts from pooled plasma and homogenized feces were profiled using a high-resolution LC-MS/MS (liquid chromatography-tandem mass spectrometry) method described in **Supplemental Table S1**. After the column, the eluent was split: (1) part of the flow was used to generate on-line high-resolution MS (and/or the data-dependent MS/MS spectrum); and (2) the other part of the flow was collected for off-line AMS analysis. For each chromatogram a total of 154 fractions were collected (0-14 minutes, 6-second fractions; 14-28 minutes, 1-minute fractions).

AMS Analysis. To each fraction from 0-14 minutes, additional carbon-12 was added (paracetamol in methanol) and the whole fraction was transferred to a tinfoil cup, dried under a stream of nitrogen, and subsequently placed in the elemental analyzer, which acted as autosampler and combustion device for the AMS. To each fraction from 14-28 minutes, additional carbon-12 was added to obtain a suitable amount of carbon for AMS analysis. An aliquot of 60 μL was transferred to a tinfoil cup, dried under a stream of nitrogen, and subsequently placed in the elemental analyzer, which acted as autosampler and combustion device for the AMS.

Metabolite Identification. The Q Exactive mass spectrometer operated in the positive electrospray ionization mode. The heated electrospray ion source voltage was 3.0 kV. The heated

capillary temperature was 350 °C. Auxiliary and spare gases were set to 20 and 0 units, respectively. The scan-event cycle consisted of a full-scan mass spectrum (100-1000 m/z) at a resolving power of 35,000 and the corresponding data-dependent tandem mass spectrometry (MSn) scans were acquired at a resolving power of 35,000. Accurate mass measurements were performed using external calibration. A reference list of known metabolites of abrocitinib and their expected molecular ions was added to an inclusion list to prioritize those ions during data acquisition. Post-acquisition searching of LC-MSn data for molecular ions representing possible metabolites of ^{14}C abrocitinib was performed manually. In addition, the LC-MS data associated with every radiochromatographic peak was also interrogated. LC-MS peaks identified to be possible metabolites, based on the molecular ions, were compared against blank samples. In cases where the signal strength was of sufficient intensity to trigger MSn scanning, the subsequent MS2 spectra were examined to further confirm the identity and structure of possible metabolites. In addition, LC-MS chromatograms were compared directly against the appropriate predose matrix chromatogram to identify additional metabolite peaks.

Chiral Separation of Metabolites M2 and M3. Plasma, urine, and feces homogenate extracts were injected in triplicate using the UHPLC system described above (**Supplemental Table S1**) and the fraction containing both enantiomers was collected. For each matrix these 3 fractions (from the triplicate injections per matrix) were pooled and dried under a stream of nitrogen. The dried fractions were reconstituted in 200 μL mobile phase (0.1% trifluoroacetic acid,0.1% isopropylamine in acetonitrile:methanol (90:10 % v/v)). The reconstituted fractions were injected on the UHPLC where the chromatography was performed using a ChiralPAK ZWIX(-) (4×150 mm, 3 μm, Diacel, Chiral Technologies, Inc., West Chester, PA). An isocratic flow rate of 0.25 mL/min was maintained throughout the analysis. For each matrix a duplicate

14

injection of 25 µL was performed. After the column, the eluent was fraction collected for off-line

AMS analysis.

Isolation of Metabolites M6 and M7. Approximately 30 mL of 0-24 hour pooled human

urine was centrifuged at 1800*g* for 20 minutes and the supernatant applied to a Bond Elut C-18

SPE cartridge (10 gm, Agilent Technologies, Santa Clara, CA) equilibrated in 5% methanol in

water at a flow rate of 2.0 mL/min. The cartridge was successively eluted with 50 mL of 10 mM

ammonium acetate in water containing varying percentages of 1:1 methanol:acetonitrile (2.5, 5,

10, 15, 20, 25, 30, and 2.5%). 50 µL of the flow-through and each eluate were analyzed by LC-

MS/MS (**Supplemental Table S2**) to determine which fractions contained metabolites M6 and

M7. Eluates rich in M6 and M7 were evaporated to near dryness in a vacuum centrifuge at room

temperature. Residues were re-dissolved in 0.1% formic acid in 1:1 methanol:acetonitrile

(97.5:2.5 % v/v) and 5-mL aliquots were fractionated using the LC-MS/MS method shown in

Supplemental Table S3. 1.0 minute fractions were collected and 10 µL of fractions between 9.0

and 36 minutes were analyzed by LC-MS/MS for presence of M6 and M7 metabolites

(**Supplemental Table S4**). Fractions rich in M6 and M7 were pooled and evaporated to dryness

in a vacuum centrifuge at room temperature. The residues were re-dissolved in 1.0 mL 10 mM

ammonium acetate:methanol:acetonitrile (97.5:1.25:1.25 % v/v) and purified using the LC-

MS/MS method shown in **Supplemental Table S5**. 1.0-minute fractions were collected and 10

µL of fractions between 4.0 minutes and 32 minutes were analyzed by LC-MS/MS

(**Supplemental Table S4**) for presence of m/z 354 (M7) and m/z 370 (M6) metabolites.

Fractions containing metabolites were then pooled and evaporated to dryness for nuclear

magnetic resonance (NMR) analysis.

15

Nuclear Magnetic Resonance Characterization of Metabolite M6 and M7. All samples were dissolved in 0.05 mL of DMSO-d6 "100%" (Cambridge Isotope Laboratories, Andover, MA) and placed in a 1.7 mm NMR tube in a dry argon atmosphere. ^{1}H and ^{13}C spectra were referenced using residual DMSO-d6 (2.50 ppm relative to TMS, δ=0.00, 13C δ=39.50 ppm relative to TMS, δ=0.00). NMR spectra were recorded on a Bruker Avance 600 MHz (Bruker BioSpin Corporation, Billerica, MA) controlled by Topspin V3.1 and equipped with a 1.7 mm TCI Cryo probe. 1D spectra were recorded using a sweep width of 10,000 Hz and a total recycle time of 7 s. The resulting time-averaged free induction decays were transformed using an exponential line broadening of 1.0 Hz to enhance signal to noise. The 2D data were recorded using the standard pulse sequences provided by Bruker. At minimum a 1K × 128 data matrix was acquired using a minimum of 2 scans and 16 dummy scans with a spectral width of 10,000 Hz in the f2 dimension. The data was zero-filled to at least 1K data point.

Abrocitinib Quantification. Plasma samples from Period B were analyzed for abrocitinib concentration at WuXi AppTec (Shanghai, China) with a validated LC-MS/MS method. Abrocitinib and internal standard PF-06651703 (deuterated abrocitinib) were extracted from 75 μL human plasma using liquid-liquid extraction with ethyl acetate and extracts were analyzed with the LC-MS/MS method shown in **Supplemental Table S6**. The calibration range was 1.00-2000 ng/mL, and the QC concentrations were 3.00, 60.0, 1000, and 1600 ng/mL. The interday assay accuracy ranged from –4.8% to 0.0% and the between-day precision was ≤7.8%.

Plasma samples from Period B were analyzed for ^{14}C-abrocitinib concentration at TNO (Microbiology and Systems Biology, Ziest, Netherlands) using a qualified analytical method. Protein precipitation of 100 μL plasma was performed using 3:1 acetonitrile:plasma followed by centrifugation, drying under a stream of nitrogen, and reconstitution with 80:10:10 2 mM

16

ammonium acetate:acetonitrile:methanol. Samples were analyzed by LC-MS/MS methods (**Supplemental Table S1**) with AMS detection (1MV multi-element AMS model 4110 Bo, High Voltage Engineering) The calibration range was 0.50-100 mBq/mL and QC concentrations were 1.50, 20.0, 75.0, and 200 mBq/mL. The interday assay accuracy ranged from –10.9% to –3.0% and the between-day precision was ≤3.7%.

In Vitro CYP450 Assignment. The experimental conditions used in vitro were confirmed to yield linear reaction velocities as determined from preliminary range-finding experiments.

In Vitro Hepatocyte Fractional Metabolism. The reaction phenotyping experiment was conducted using ^{14}C abrocitinib (1 µM), pooled human cryopreserved hepatocytes at 0.75 million cells/mL in William's E Medium at 37 °C in 5% CO_2/95% air and 85% relative humidity for 30 minutes. Aliquots were quenched into acetonitrile (1:4, v/v) and centrifuged (1860 × g) for 5 minutes and the supernatant was transferred to clean 15 mL conical glass tubes. The supernatants were dried in a Genevac™ (Genevac Inc, Valley Cottage, NY) evaporative centrifuge at 37 °C and the resulting residues were reconstituted in 100 µL of 2 mM ammonium acetate:acetonitrile:methanol (95:2.5:2.5 % v/v).

Sample bioanalysis was performed using the LC-MS/MS method shown in **Supplemental Table S7**. Post-column, the eluent was split: (1) part of the flow was used to generate on-line high-resolution MS (and/or data-dependent MS/MS) spectrum; and (2) the other part of the flow was diverted to the fraction collector. Fractions were collected in 6-second intervals into Lumaplate-96 well plates (PerkinElmer, Waltham, MA) and dried in a Genevac™ evaporative centrifuge at 37 °C. Plates were then placed in a PerkinElmer MicroBeta2 counter

17

and each well counted for total ^{14}C for 5 minutes. The results were used to generate a reconstructed radiochromatogram.

Enzyme kinetics. Experiments for the determination of enzyme kinetic parameters were conducted in human liver microsomes. Abrocitinib (0.1-1000 μM) was incubated in 100 mM potassium phosphate buffer (pH 7.4) containing 3 mM MgCl$_2$, and 0.3 mg/mL microsomal protein HLM-103 at 37 °C. Reactions were initiated with NADPH (1.2 mM) immediately followed by substrate and terminated after 15 minutes by quenching aliquots of the incubation mixture with acetonitrile-containing internal standard (Diclofenac, 10 ng/mL). Samples were centrifuged (1700 g) for 10 minutes and 100 μL of supernatant was transferred to clean 96 deep-well plates. The supernatants were dried down under a stream of nitrogen and reconstituted in 100 μL of 90% water/10% acetonitrile. Incubations for enzyme kinetic determination were conducted in triplicate.

CYP Chemical Inhibition. The CYP-selective chemical inhibition experiment was conducted using abrocitinib (10 μM), pooled human hepatocytes and chemical inactivators of CYPs 1A2, 2B6, 2C8, 2C9, 2C19, 2D6, 3A and pan-CYP in a 96-well plate. Hepatocytes (120 μL) at 0.75 million cells/mL in Williams E media were preincubated with inhibitors for 15 or 30 minutes prior to initiating the reactions by the addition of abrocitinib. Incubations containing 100 μM gemfibrozil glucuronide (CYP2C8), 15 μM tienilic acid (CYP2C9), 1 mM 1-aminobenzotriazole (pan-CYP) were preincubated 30 minutes and 10 μM furafylline (CYP1A2), 5 μM PPP (2-phenyl-2-(1-piperdinyl)propane, CYP2B6), 5 μM esomeprazole (CYP2C19), 2 μM CYP3cide (CYP3A4) and 25 μM troleandomycin (CYP3A4/5) were preincubated for 15 minutes with human hepatocytes to achieve complete inactivation of respective CYP isoforms (Walsky et

18

al., 2008; Yang et al., 2016). Quinidine (10 µM) was used as a competitive inhibitor (CYP2D6) without preincubation prior to addition abrocitinib. Incubations of abrocitinib were conducted at 37 °C in 5% CO_2/95% air and 75% relative humidity for 30 minutes. Aliquots were collected into acetonitrile-containing internal standards to quench the reaction. Quenched samples were centrifuged (1700 g) for 10 minutes and 150 µL of supernatant was transferred to clean 96 deep-well plates. The supernatants were dried under a stream of nitrogen and reconstituted in 100 µL of 10% acetonitrile/90% water. Selective chemical inhibition experiments were conducted in triplicate.

Enzyme Kinetics and Chemical Inhibition Bioanalysis: Sample bioanalysis was performed using the LC-MS/MS method shown in **Supplemental Table S8**. Integration and quantitation of metabolites and internal standard molecule peak areas were performed using Analyst version 1.6.2 (AB Sciex) to derive the analyte to internal standard peak area ratios. Standard curves for the quantitation of metabolite concentrations were prepared from plots of area ratio versus concentration and analyzed using a linear regression with either 1/x or 1/x 2 weighting.

Fractional Clearance in Human Hepatocytes. To determine the fractional contributions of metabolic pathways of ^{14}C-abrocitinib, radioactivity counts for fractions were plotted against time to reconstruct LC chromatograms, which were then aligned and assessed against MS spectral data for agreement. The sum of radioactive counts associated with an individual chromatographic peak was determined and compared to the total radioactivity recovered to derive the % of total radioactivity using the 30-minute time point. The contribution of a single metabolic pathway (represented by an individual metabolite plus any secondary metabolites

deriving from it) was calculated as the response of the individual metabolite divided by the total metabolism of abrocitinib.

Enzyme Kinetics in Human Liver Microsomes. Substrate concentration (S) and velocity (V) data were fitted to the appropriate enzyme kinetic model by nonlinear least-squares regression analysis (SigmaPlot version 13; Systat Software, Inc., San Jose, CA or GraphPad version 6.03; GraphPad Software Inc., La Jolla, CA) to derive the apparent enzyme kinetic parameters using the Michaelis-Menten model (eq. 1) and the substrate inhibition model (eq. 2).

$$V = \frac{V_{max} \times S}{K_m + S} \tag{1}$$

$$V = \frac{V_{max} \times S}{K_m + S \times (1 + S/Ki)} \tag{2}$$

where V_{max} is the maximal velocity, K_m or S_{50} is the substrate concentration at half-maximal velocity, and K_i is an inhibition constant. The best fit was based on a number of criteria, including visual inspection of the data plots (Michaelis-Menten and Eadie-Hofstee), distribution of the residuals, size of the sum of the squared residuals, and the standard error of the estimates. Selection of models other than Michaelis-Menten was based on the F-test ($P < 0.05$) or the Akaike Information Criterion.

In vitro apparent intrinsic clearance (CL_{int}) values were calculated using equation 3:

$$CL_{int} = \frac{V_{max}}{K_m} \tag{3}$$

20

CL_{int} data were also calculated from rate of product formation (V) obtained at substrate concentrations (S) below the apparent K_m ([S]<K_m), in which cases eq. 1 was rearranged to CL_{int} = V/[S].

In vitro apparent intrinsic clearance ($CL_{int,app}$) and scaled in vivo apparent intrinsic clearance ($CL_{int,app,sc}$) values for M1, M2/M3, and M4 were calculated using the following equations:

$$CL_{int,app(HLM)} = \frac{V_{max}}{K_m} \qquad (4)$$

$$CL_{int,app,sc(HLM)} = CL_{int,app(HLM)} \times 45 \; mg \; protein/gram \; liver \times 21 \; g \; liver/kg \; body \; weight \quad (5)$$

Selective CYP Chemical Inhibition in Human Hepatocytes. To determine the contribution of each CYP isoform to abrocitinib metabolism in human hepatocytes, the metabolite formation rates were calculated by dividing the metabolite concentration by incubation time and protein concentration. The effect of CYP selective chemical inhibitors on the formation rate of each metabolite was calculated using the following formula:

$$\% \; Inhibition \; (unscaled) = (1 - \frac{v_{inh}}{v_{ctrl}}) \times 100 \qquad (6)$$

wherein v_{inh} is the rate of formation in the presence of inhibitor and v_{ctrl} is the rate of metabolite formation in the control human hepatocyte incubation. To determine the contribution of each CYP isoform for the metabolites without standard, the analyte to internal standard area ratio was used. When the combined inhibitor effects on a metabolic pathway totaled more than 100%, the percentage inhibition values for that pathway were normalized to 100%. The fraction of

21

abrocitinib metabolism represented by a single metabolite x and specific CYP isoform z

($f_{mMx,CYPz}$) was calculated using the following equation:

$$f_{mMxCYPz} = \frac{\%inhibition}{100} \times f_{CL}$$

(7)

where % inhibition is the scaled inhibition of metabolite x by a CYP specific inhibitor z and f_{CL}

is the fraction of abrocitinib clearance represented by metabolite x determined in radiolabeled

human hepatocyte experiments.

A statistical analysis was conducted comparing the metabolite formation rates in the

presence of inhibitor versus control incubations to confirm significance. A one-way analysis of

variance analysis with a Dunnett's Test for multiple comparisons was applied to the triplicate

values from inhibited and control conditions.

In Vitro Pharmacology. The potency of abrocitinib and its metabolites against the four

JAK isoforms, JAK1, JAK2, JAK3, and TYK2, was measured in terms of half-maximal

inhibitory concentration (IC_{50}) as previously reported (Dowty et al, 2019). In addition, the

potency of abrocitinib and its metabolites to inhibit the ability of various cytokines to induce

signal transducer and activator of transcription (STAT) phosphorylation in human whole blood,

human keratinocytes or human acute monocytic leukemia (THP-1) cells was assessed as

previously reported (Dowty et al., 2019). More methodology details are provided in the

Supplementary Methods.

Plasma protein binding. An equilibrium dialysis method was used to determine plasma

fraction unbound (f_u) values, as described previously (Riccardi et al., 2017). Briefly, dialysis

membranes (MWCO 12-14K) and 96-well dialysis devices were assembled following the

22

manufacturer's instructions (HTDialysis, LLC, Gales Ferry, CT, USA). Human plasma samples (pooled mixed sex; BioIVT, www.bioivt.com) containing 1 µM test compounds with 1% DMSO were dialyzed against PBS for 6 hours in a humidified incubator (75% relative humidity; 5% CO_2/95% air) at 37 °C with shaking at 450 RPM. Quadruplicates of binding were measured for each compound. Samples were matrix-matched and quenched with cold acetonitrile containing internal standard(s). The solutions were centrifuged ($3600g$, 30 minutes, 4°C), and the supernatant was analyzed using a generic LC-MS/MS method **(Supplemental Tables S9-S11)**.

Blood-to-plasma ratio. Human blood-to-plasma ratio was measured by Unilabs York Bioanalytical Solutions (York, UK). Test compounds were incubated in quadruplicate with fresh human blood (mixed sex, at least 1 sample per sex, Clinical Trials Laboratory Services Ltd, London, UK) at 1 µM in a humidified incubator (95% relative humidity; 5% CO_2/95% air) for 1 and 3 hours at 37°C with shaking at 450 RPM. Following incubation, plasma samples were obtained by centrifuging blood samples ($3000g$, 7 minutes). Both plasma and blood samples were matrix-matched with each other and quenched with acetonitrile-containing internal standard. The solutions were centrifuged and the supernatant was analyzed using a generic LC-MS/MS method (**Supplemental Tables S9-S11**). Peak area ratios were used to calculate blood-to-plasma ratio.

Results

Clinical Safety. All 6 participants completed the study. Oral and IV doses of abrocitinib in Period A and B were safe and well tolerated and no serious or drug-related adverse events were reported. All reported adverse events were mild in severity (**Supplemental Table S12**), and there were no clinically relevant changes in vital signs, clinical laboratory test results, or electrocardiogram measurements throughout the study period.

Pharmacokinetics. Plasma concentration–time profiles and pharmacokinetic parameters of abrocitinib are summarized in **Fig. 1** and **Table 1**, respectively. Abrocitinib showed rapid absorption following oral administration with a T_{max} of 0.5 hour. Systemic clearance and volume of distribution of abrocitinib were estimated at 64.2 L/h and 100 L, respectively. The absorption and elimination profiles of total radioactivity were comparable to those of abrocitinib, with >97% of circulating radioactivity measured within the 0 to 12-hour collection pool. There were some differences in CYP450 genotypes with 3 participants with 2C19*1/*1 (extensive metabolizer [EM]) and 2C9*1/*1 (EM); 2 participants with 2C19*1/*17 (rapid metabolizer [RM]) and 2C9*1/*2 (intermediate metabolizer); and 1 participant with 2C19*1/*17 (RM) and 2C9*1/*1 (EM). However, these differences did not translate into significant differences in systemic clearance as percentage coefficient of variation was only 14%.

Disposition and Metabolite Profiles. After a single oral dose of ^{14}C-abrocitinib in male participants, radioactivity was excreted predominantly in the urine (**Fig. 2**). At 240 hours after the dose, the mean (± standard deviation) cumulative excretion in the urine was 85.0% (± 6.0%) and in the feces was 9.5% (± 0.5%) (**Table 2**). In total, 94.5% (± 5.9%) of the radioactive dose was recovered in urine and feces, with a major portion of excreted radioactivity recovered during the first 24 hours after dosing (urine 84.0% [± 6.4%], feces 1.7% [± 3.0%], total 85.7% [±

24

8.7%]). Collectively, 13 metabolites were identified in urine and feces (**Table 2**). Oxidative

metabolites M6, M1, M2, and M4 were the most abundant in urine at 12.2%, 16.2%, 13.5%, and

15.4% of the administered dose, respectively. All other metabolites comprised less than 10% of

the dose. Representative HPLC radiochromatograms of plasma (0- to 12-hour pool after dose,

representing >97% radioactivity AUC), urine (0- to 12-hour pool after dose, representing 96% of

urine total recovery), and fecal (pools representing 97% of the feces total recovery) profiling are

shown in **Fig. 3**. Unchanged abrocitinib accounted for the majority (25.8%) of the total

circulating radioactivity (**Table 2**) with M1, M2, and M4 contributing 11.3%, 12.4%, and 13.8

%, respectively. All remaining circulating metabolites made up less than 10% each of total

circulating radioactivity.

Metabolite Identification. Structural determination was performed on 13 metabolites of

abrocitinib. Metabolites were identified by comparing retention times on chromatograms and

mass spectra of authentic standards or elucidated based on mass fragmentation patterns (**Table 3**

and **Supplemental Table S13**). The proposed metabolic pathways of abrocitinib are shown in

Fig. 4.

The parent compound, abrocitinib, had a retention time of 11.5 minutes using the HPLC

conditions described. Abrocitinib has a protonated molecular ion at m/z 324.1490 (molecular

formula $C_{14}H_{21}N_5O_2S$, theoretical mass m/z 324.1489). Its MS/MS spectrum showed diagnostic

fragment ions at m/z 201, 176, 175, 149, and 70. The ion at m/z 201 resulted from the neutral

loss of the propane-1-sulfonamide. Fragment m/z 176 represented the N-cyclobutylpropane-1-

sulfonamide. Fragmentation through the cyclobutane ring yielded m/z 175. Fragment m/z 149,

N-methyl-7H-pyrrolo[2,3- d]pyrimidin-4-amine, resulted from the neutral loss of N

cyclobutylpropane-1-sulfonamide, whereas fragment m/z 70 represented the cyclobutanamine

ion.

Metabolite M6. M6 is a minor metabolite in plasma (3.4% of the radioactivity in the

circulation) and was identified in urine (14.7%) and in fecal homogenate (8.3%) from profiled

radioactivity. The amount of dose excreted as M6 in urine and fecal homogenate was 12.2% and

0.8%, respectively. M6 (molecular formula $C_{14}H_{19}N_5O_5S$, theoretical mass m/z 370.1180,

observed mass m/z 370.1179), was 46 mass units greater than parent and had a retention time of

3.4 minutes on HPLC. Fragmentation of the molecular ion yielded m/z 217, 165, and 70.

Fragment m/z 217 represented the neutral loss of propane-1-sulfonamide and the addition of 16

mass units to the N-cyclobutyl-N-methyl-7H-pyrrolo[2,3-d]pyrimidin-4-amine. Fragment m/z

70, cyclobutanamine, remained intact. The remaining increase of 30 mass units was suggested to

occur on the propane through di-oxidation and reduction.

NMR analysis of M6 (**Supplemental Fig. S1**) isolated from pooled 0- to 12-hour human

urine supported formation of a carboxylic acid on the methyl group of the propyl side chain; it

also supported formation of an amide carbonyl and a methylene at the 6' and 5' positions of the

pyrrolo pyrimidine ring, respectively. The methyl group was absent in the 1H spectrum of M6; in

the homonuclear correlation spectroscopy (COSY) spectrum, cross peaks were observed between

positions H18 (δ = 3.07 ppm) and H21 (δ = 2.31 ppm). Formation of the acid was further

confirmed in the Heteronuclear Multiple Bond Correlation (HMBC) spectrum, which revealed

cross peaks from both H18 and H21 into a carbon with a chemical shift value of 172.5 ppm,

likely corresponding to the acid carbonyl (C22). Methines corresponding to the 6' and 5'

positions of the pyrrolo pyrimidine ring were both absent in the 1H spectrum of M6 and a new

methylene at the 5' position (1H/ 13C δ = 3.8/35.6 ppm) was observed. The HMBC spectrum

26

revealed a cross peak between the newly formed methylene at the 5' position (H9) into a carbon

resonance at 175.2 ppm, suggesting the presence of an amide carbonyl at the 6' position (C8).

Additional cross peaks in both COSY and HMBC spectra as well as resonances observed in the

heteronuclear single quantum coherence spectrum (data not shown) indicated the rest of the

molecule remained unmodified with respect to parent drug.

Metabolite 340-5. 340-5 was defined as a minor metabolite in plasma (1.0% of the

radioactivity in the circulation). The amount of dose excreted as 340-5 in urine and fecal

homogenate was 0.4 % and 0.2%, respectively. The deformylated carboxylic acid metabolite,

340-5 (molecular formula $C_{13}H_{17}N_5O_4S$, theoretical mass m/z 340.1074, observed mass m/z

340.1074), was 16 mass units greater than parent and had a retention time of 4.9 minutes on

HPLC. Fragmentation of the molecular ion yielded m/z 296, 218, 201, 175, 149, and 70.

Fragment m/z 296 represented the neutral loss of 44 atomic mass units, which is diagnostic for

the loss of COOH from the remaining ethane group. All other fragments were identical to the

parent compound. Fragment m/z 218 represents the intact N-methyl-N-(7H-pyrrolo[2,3-

d]pyrimidin-4-yl)cyclobutane-1,3-diamine portion of the molecule. All other fragments were

identical to the parent compound.

Metabolite 372-1. 372-1 is a minor metabolite in plasma (2.5% of the radioactivity in the

circulation). The amount of dose excreted as 372-1 in urine and fecal homogenate was 0.7 % and

0.2%, respectively. The tri-hydroxylated metabolite, 372-1 (molecular formula $C_{14}H_{21}N_5O_5S$,

theoretical mass m/z 372.1336, observed mass m/z 372.1334), was 48 mass units greater than

parent and had a retention time of 5.0 minutes on HPLC. Fragmentation of the molecular ion

yielded m/z 176 and 70. Fragment m/z 176 represented the intact N cyclobutylpropane-1-

sulfonamide, indicating that each oxidation was taking place on the N-methyl-7H-pyrrolo[2,3-d]pyrimidin-4-amine.

Metabolite M7. M7 was defined as a minor metabolite in plasma (4.6% of the radioactivity in the circulation). The amount of dose excreted as M7 in urine and fecal homogenate was 5.6% and 1.5%, respectively. The carboxylic metabolite, M7 (PF-06737821, 354-1) (molecular formula $C_{14}H_{19}N_5O_4S$, theoretical mass m/z 354.1231, observed mass m/z 354.1230), was 30 mass units greater than parent and had a retention time of 5.2 minutes on HPLC. Fragmentation of the molecular ion yielded m/z 218, 201, 175, 149, and 70. Fragment m/z 201 represented unchanged N-cyclobutyl-N-methyl-7H-pyrrolo[2,3-d]pyrimidin-4-amine. NMR analysis of M7 (**Supplemental Fig. S2**) isolated from pooled 0- to 12-hour human urine supported formation of a carboxylic acid on the methyl group of the propyl side chain. The methyl group was absent in the 1H spectrum of 354-1, whereas in the COSY spectrum cross peaks were observed between positions H18 ($\delta = 3.12$ ppm) and H21 ($\delta = 2.40$ ppm). Formation of the acid was further confirmed in the HMBC spectrum, which revealed cross peaks from both H18 and H21 into a carbon with a chemical shift value of 172.5 ppm, likely corresponding to the acid carbonyl (C22). Additional cross peaks in both COSY and HMBC spectra as well as resonances observed in the heteronuclear single quantum coherence spectrum (data not shown) indicated the rest of the molecule remained unmodified with respect to parent drug.

Metabolite M8. M8 is a minor metabolite in plasma (1.4% of the radioactivity in the circulation). The amount of dose excreted as M8 in urine was 1.3%. The di-hydroxylated metabolite, M8 (PF-07055039, 356-1) (molecular formula $C_{14}H_{21}N_5O_4S$, theoretical mass m/z 356.1387, observed mass m/z 356.1387), was 32 mass units greater than parent and had a retention time of 5.8 minutes on HPLC. Fragmentation of the molecular ion yielded m/z 217,

165, and 70, which represented the proposed hydroxylation of the 7H-pyrrolo[2,3-d]pyrimidin-4-ylium group. The remaining hydroxylation was proposed to be located on the propyl group. Fragmentation was identical to the synthetic reference standard.

Metabolite 358-1. 358-1 was defined as a minor metabolite in plasma (2.0% of the radioactivity in the circulation). The amount of dose excreted as 358-1 in urine and fecal homogenate was 1.1 % and 0.1%, respectively. 358-1 (molecular formula $C_{14}H_{23}N_5O_4S$, theoretical mass m/z 358.1544, observed mass m/z 358.1543) was 34 mass units greater than parent, which represented the result of hydroxylation and hydrolysis. It had a retention time of 6.1 minutes on HPLC. Fragmentation of the molecular ion yielded m/z 217, 176, 165, and 70. Fragment m/z 176 represented the intact N-cyclobutylpropane-1-sulfonamide. Fragment m/z 183 represented the N-methyl-7Hpyrrolo[2,3-d]pyrimidin-4-amine with the addition of 34 mass units. The ions m/z 217 and 165 represented the loss of water and dehydration with the intact hydroxyl group on the 7H-pyrrolo[2,3-d]pyrimidin-4-ylium group.

Metabolite 356-1a. 356-1a was defined as a minor metabolite in plasma (1.5% of the radioactivity in the circulation). The amount of dose excreted as 356-1a in urine and fecal homogenate was 1.7% and 0.2%, respectively. The di-hydroxylated metabolite, 356-1a (molecular formula $C_{14}H_{21}N_5O_4S$, theoretical mass m/z 356.1387, observed mass m/z 356.1386), was 32 mass units greater than parent and had a retention time of 6.4 minutes on HPLC. Fragmentation of the molecular ion yielded m/z 217, 191, 165, and 70. The ion m/z 165 represented the proposed hydroxylation of the 7H-pyrrolo[2,3-d]pyrimidin-4-ylium group. The ion m/z 192 represented the proposed hydroxylation of the N-cyclobutylpropane-1-sulfonamide group.

Metabolite 356-2. 356-2 was defined as a minor metabolite in plasma (1.5% of the radioactivity in the circulation). The amount of dose excreted as 356-2 in urine and fecal homogenate was 3.3% and 0.6%, respectively. The di-hydroxylated metabolite, 356-2 (molecular formula $C_{14}H_{21}N_5O_4S$, theoretical mass m/z 356.1387, observed mass m/z 356.1385), was 32 mass units greater than parent and had a retention time of 6.5 minutes on HPLC. Fragmentation of the molecular ion yielded m/z 233, 207, 181, and 70. The ions m/z 233 and 181 represented the proposed di-hydroxylation of the 7H-pyrrolo[2,3-d]pyrimidin-4-ylium group.

Metabolite M1. M1 was defined as a major metabolite in plasma (11.3% of the radioactivity in the circulation). The amount of dose excreted as M1 in urine and fecal homogenate, was 16.2% and 1.7%, respectively. The hydroxylated metabolite, M1 (molecular formula $C_{14}H_{21}N_5O_3S$, theoretical mass m/z 340.1438, observed mass m/z 340.1438), was 16 mass units greater than parent and had a retention time of 7.6 minutes on HPLC. Fragmentation of the molecular ion yielded ions m/z 218, 175, 149, and 70, all identical to the parent molecule. Fragmentation was identical to the synthetic reference standard.

Metabolite M2. Both M2 and M3 are coeluting enantiomers. The abundance of the individual enantiomers was determined using both UHPLC and chiral chromatography. M2 was defined as a major metabolite in plasma (12.4% of the radioactivity in the circulation). The amount of dose excreted as M2 in urine and fecal homogenate was 13.5% and 0.5%, respectively. Hydroxylated M2 (molecular formula $C_{14}H_{21}N_5O_3S$, theoretical mass m/z 340.1438, observed mass m/z 340.1438) and M3 (molecular formula $C_{14}H_{21}N_5O_3S$, theoretical mass m/z 340.1438) are 16 mass units greater than parent. M2 had a retention time of 8.5 minutes on HPLC. Fragmentation of the molecular ion yielded ions m/z 201, 175, 149, and 70,

which are all identical to the parent molecule. Fragmentation was identical to the synthetic reference standard.

Metabolite M3. M3 was defined as a minor metabolite in plasma (4.8% of the radioactivity in the circulation). The amount of dose excreted as M3 in urine and fecal homogenate was 4.5% and 0.3%, respectively. Fragmentation of the molecular ion yielded ions m/z 201, 175, 149, and 70, all identical to the parent molecule. Fragmentation was identical to the synthetic reference standard.

Metabolite M4. M4 was defined as a major metabolite in plasma (13.8% of the radioactivity in the circulation). The amount of dose excreted as M4 in urine and fecal homogenate was 15.4% and 0.3%, respectively. The oxidized metabolite, M4 (PF-07054874, 340-4), (molecular formula $C_{14}H_{21}N_5O_3S$, theoretical mass m/z 340.1438, observed mass m/z 340.1438) was 16 mass units greater than parent. This metabolite co-eluted with M5. It had a retention time of 10.0 minutes on HPLC. Fragmentation of the molecular ion yielded m/z 217, 191, 176, 165, and 70. Fragmentation was identical to the synthetic reference standard.

Metabolite M5. M5 was defined as a minor metabolite in plasma (0.4% of the radioactivity in the circulation). The amount of dose excreted as M5 in urine was 0.3% and was not detected in fecal homogenate. The N-desmethylated metabolite, M5, (molecular formula $C_{13}H_{19}N_5O_2S$, theoretical mass m/z 310.1332, observed mass m/z 310.1332) was 14 mass units less than parent, and had a retention time of 10.0 minutes on HPLC. This metabolite co-eluted with M4. Fragmentation of the molecular ion yielded m/z 187, 161, and 135 (**Table 3**). Fragmentation was identical to the synthetic reference standard. The abundance of co-eluting M4 and M5 were determined using the mass spectrometry, peak areas of reference standards at a

31

single concentration. These peak areas were used to calibrate the abundance of M4 and M5 in the pooled plasma, urine, and feces sample extract profiles. The estimated mass ratio of M4 to M5 was determined to be 38.4, 49.4, and 13.3 for pooled plasma, urine, and fecal homogenate extracts, respectively. The combined [^{14}C] peak area for the pooled plasma extracts, pooled urine, and pooled fecal homogenate extracts was 14.2, 19.2, and 3.6%, respectively. The calculated individual contribution of [^{14}C] peak area for each metabolite (M4/M5) in pooled plasma extracts was 13.8/0.4%, in pooled urine, 18.8/0.4%, and in pooled fecal homogenate extracts, 3.3/0.3%.

CYP Phenotyping. The primary metabolites of abrocitinib were quantitated following a 30-minute incubation of ^{14}C-abrocitinib with human hepatocytes for determination of fractional contribution to total clearance. The resulting radiochromatogram is presented in **Supplemental Fig. S3** and the percentage of total radioactivity associated with the formation of metabolites is presented in **Table 4**. Based on the percentage of total radioactivity observed at the 30-minute time point, the respective fractional clearance (f_{CL}) values were 0.390 for M1, 0.288 for M2/M3, 0.247 for M4, 0.0240 for M7, 0.011 for 358-1 0.011 for 372-1, and 0.0291 for 149. Since M7 is likely a secondary metabolite of M1 (**Fig. 4**), the contribution of M7 metabolism was combined into the M1 route. Metabolites 358-1 and 372-1 are likely secondary metabolites of M4 (**Fig. 4**), therefore the contributions were combined into the M4 route. The final f_{CL} values for the 4 metabolic pathways characterized were 0.414 for M1, 0.288 for M2/M3, 0.269 for M4, and 0.0291 for 149. The proportion of metabolism attributed to CYP activity from these 4 pathways totaled 1.0.

Enzyme kinetic parameters and intrinsic clearance values determined for the formation of M1, M2/M3, and M4 from abrocitinib metabolism in human liver microsomes are listed in **Table**

5 and associated data are presented graphically in **Supplemental Fig. S4**. Kinetic parameters for

metabolite 149 could not be determined. Visual inspection of the Eadie-Hofstee plots for the M1,

M2/M3, and M4 reaction rate data demonstrated nonlinear profiles consistent with substrate

inhibition. For all 3 metabolites, a Michaelis-Menten equation with substrate inhibition was

selected for the determination of enzyme kinetic parameters. Based on these kinetic parameters,

the respective M1, M2/M3, and M4 $CL_{int,app}$ values were 0.187, 0.294, and 1.70 µL/min/mg and

$CL_{int,app,sc}$ values were 0.176, 0.278, and 1.60 mL/min/kg. The total $CL_{int,app,sc}$ of three major

metabolites for abrocitinib was 2.05 mL/min/kg.

The results of CYP selective chemical inhibition on the metabolism of abrocitinib in

human hepatocytes are presented in **Table 6**. The metabolic formation rates of M1, M2/M3, and

M4 were primarily inhibited in the presence of PPP (2B6), tienilic acid (2C9), esomeprazole

(2C19), and troleandomycin (3A). After scaling, formation of metabolite M1 was inhibited 16%

by PPP (2B6), 24% by tienilic acid, 52% by esomeprazole, and 8.0 % by troleandomycin.

Formation of metabolite M2/M3 was inhibited 45% by tienilic acid and 55% by esomeprazole.

M4 was inhibited 25% by tienilic acid, 57% by esomeprazole, and 18% by troleandomycin. A

summary of the abrocitinib CYP assignment is presented in **Table 6**. After normalizing for f_{CL}

for each metabolic pathway, the fraction of metabolic clearance of abrocitinib catalyzed by

CYP2C19, 2C9, 3A4, and 2B6 were 0.53, 0.30, 0.11, and 0.066, respectively.

In Vitro Pharmacology. The enzyme potency of abrocitinib and the oxidative

metabolites M1, M2, and M4 was assessed against four JAK isoforms using enzymatic assays at

1 mM adenosine triphosphate (**Table 7**). Abrocitinib was more potent against JAK1 vs JAK2 or

TYK2 and demonstrated little potency for JAK3 (IC_{50} >10,000 nM). M1 and M2 exhibited a

similar potency and selectivity profile as abrocitinib. The IC_{50} values for M4 with all 4 JAK

isoforms were >10,000 nM. Therefore, the circulating metabolites M1 and M2 are active metabolites that may contribute to the overall pharmacology of abrocitinib, whereas M4 is pharmacologically inactive.

The cellular potency of abrocitinib, M1, and M2 was evaluated by measuring the inhibition of phosphorylation of STATs following stimulation with various cytokines in human whole blood (represented as total and unbound IC_{50}), human keratinocytes, and THP-1 cells (IC_{50} values considered unbound) (**Table 8**). Abrocitinib was much more potent against cytokines that transduce their signals via JAK1-dependent pathways with IC_{50} values ranging from 40.0 nM for IL-31-induced STAT3 phosphorylation to 1690 nM (unbound 569 nM) for IFNγ-induced STAT1 phosphorylation when compared to cytokines that transduce signals via JAK1-independent pathways with IC_{50} values ranging from 7180 nM (unbound 2420 nM) for EPO-induced STAT5 phosphorylation to >16,500 nM (unbound >5550 nM) for IL-23-induced STAT3 phosphorylation. Like abrocitinib, M1 and M2 inhibited JAK1-dependent signaling pathways more potently than JAK1-independent signaling pathways. In addition, the relative selectivity or potency rank order across cytokine inhibition was similar between abrocitinib, M1, and M2.

The fraction unbound in plasma for each active drug species was determined to be 0.36 for abrocitinib, 0.63 for M1, and 0.71 for M2. The blood/plasma ratios for each drug species were determined to be 1.07 for abrocitinib, 1.13 for M1, and 1.27 for M2. Blood binding parameters were used to convert whole blood pharmacology potency values into unbound values (**Table 8**).

Discussion

In this report, the pharmacokinetics and metabolism of abrocitinib were evaluated in healthy human participants. Recovery of the radiolabeled dose was ~95% indicating that the disposition of abrocitinib was well characterized. Oral absorption of abrocitinib was >90% and rapid with peak concentrations observed at ≈0.5 hour, despite being identified as an MDR1 and BCRP efflux substrate. Absolute oral bioavailability was determined to be ~60% and elimination $t_{1/2}$ ~2 hour. Systemic clearance was observed to be 64.2 L/h and steady state volume of distribution was 100 L. Clinical experience with abrocitinib has shown dose-proportional oral pharmacokinetics over a range of 30 to 400 mg, which supports linearity of parent and metabolite profiles. The $t_{1/2}$ of both abrocitinib and total radioactivity profiles was similar, indicating formation rate limited kinetics of metabolites. Following a single oral dose of abrocitinib, the major circulating component of drug-related material in plasma was abrocitinib (~26%), followed by 3 mono-hydroxylated metabolites (M1, M2, and M4) at >10%. However, following multiple daily dosing of abrocitinib to steady state, analytical measurement of metabolites indicated that M2 and M4 were observed at >10%, with M1 being considered minor at <10% (data on file).

Disposition profiles indicated oxidative metabolism as the major pathway of clearance for abrocitinib, whereas the renal route of elimination was minor at <1%. All the metabolites of abrocitinib were consistent with oxidative CYP450 metabolism with no observed evidence of direct conjugative mechanisms. In vitro phenotyping indicated multiple CYP enzymes involved in the metabolism of abrocitinib with hepatic f_m assignments of 0.53 for CYP2C19, 0.30 for CYP2C9, 0.11 for CYP3A4, and ~0.06 for CYP2B6. These in vitro results are in agreement with the impact of strong CYP2C19 inhibition by fluvoxamine and fluconazole on the exposure of co-

35

administered abrocitinib (Wang X et al., 2022). Collectively, a mass balance model was assembled for abrocitinib and is shown in **Fig. 5**.

In contrast to abrocitinib, renal elimination was observed as the major pathway of excretion for metabolites. The f_m of renal elimination was estimated to be 0.74 for M1, 0.94 for M2, and 0.93 for M4 based on clinical observation (Wang EQ et al., 2021a). Active renal clearance was predicted to be >80% for each of the metabolites, with the balance from passive filtration (f_u × glomerular filtration rate), based on estimates of metabolite exposure in plasma and total amount excreted in urine (total renal clearance = mass in urine/AUC). In vitro profiling showed that each of the primary metabolites was a substrate for the OAT3 transporter (internal data). A clinical study with the OAT3 inhibitor probenecid and co-administered abrocitinib showed an AUC_{inf} increase of approximately 2-fold for each of the metabolites in plasma (M1 1.8-fold; M2 2.2-fold; M4 2.2-fold) (Wang X et al., 2022).

Abrocitinib and its metabolites M1 and M2 were pharmacologically active at inhibiting cytokine signaling through JAK1 heterodimer pairs (ie, JAK1/JAK2, JAK1/TYK2, and JAK1/JAK3), whereas M4 was inactive. The relative JAK selectivity was similar among abrocitinib, M1, and M2. Clinical assessment of the contribution of abrocitinib, M1, and M2 to circulating plasma pharmacology based on steady-state AUC and relative potency (Leclercq et al., 2009) indicated respective percentages of ~60%, ~10%, and ~30% (data on file). Dose adjustment of abrocitinib in the context of drug-drug interaction and in special populations (renal/hepatic impairment) will be based on the total contribution of abrocitinib, M1, and M2 pharmacology (i.e., total active moiety) (Wang et al., 2021a; Wang et al., 2021b; Wang X et al., 2022).

In summary, these study results provide an important and comprehensive characterization of abrocitinib pharmacokinetics, metabolism, and clearance mechanisms as well as disposition and pharmacology of major metabolites. Furthermore, the disposition characterization of abrocitinib and its major metabolites has been consistent with clinical experience in drug-drug interaction studies and special populations.

Author Contributions

Participated in research design: Bauman, Doran, King-Ahmad, Sharma, Walker, J. Lin, T.H. Lin, Telliez, Tripathy, Goosen, Banfield, Malhotra, Dowty

Conducted experiments: Bauman, Doran, King-Ahmad, Sharma, Walker, J. Lin, T.H. Lin, Telliez, Tripathy

Contributed new reagents or analytic tools: None

Performed data analysis: Bauman, Doran, King-Ahmad, Sharma, Walker, J. Lin, Tripathy, Goosen, Banfield, Dowty

Wrote or contributed to the writing of the manuscript: Bauman, Doran, T.H. Lin, Tripathy, Goosen, Banfield, Dowty

Conflict of interest

All authors are employees and shareholders of Pfizer Inc.

Data sharing statement

Upon request, and subject to review, Pfizer will provide the data that support the findings of this study. Subject to certain criteria, conditions and exceptions, Pfizer may also provide access to the related individual de-identified participant data. See https://www.pfizer.com/science/clinical-trials/trial-data-and-results for more information.

Footnotes

All authors are full-time employees of Pfizer Inc. The authors have no conflicts of interest that are directly relevant to this study. This was a Pfizer sponsored study and the work received no external funding.

Reprint requests to:

Martin E. Dowty

Pfizer Inc.

1 Portland Street

Cambridge, MA 02139

Email: martin.dowty@pfizer.com

References

Akada H, Akada S, Hutchinson RE, Sakamoto K, Wagner KU, and Mohi G (2014) Critical role of Jak2 in the maintenance and function of adult hematopoietic stem cells. *Stem Cells* **32**:1878-1889.

Bieber T, Simpson EL, Silverberg JL, Thaçi D, Paul C, Pink AE, Kataoka Y, Chu CY, DiBonaventura M, Rojo R, Antinew J, Ionita I, Sinclair R, Forman S, Zdybski J, Biswas P, Malhotra B, Zhang F, Valdez H, and JADE COMPARE investigators (2021) Abrocitinib versus placebo and dupilumab for atopic dermatitis. *N Engl J Med* **384**:1101-1112.

Dowty ME, Lin TH, Jesson MI, Hegan M, Martin DA, Katkade V, Menon S, and Telliez JB (2019) Janus kinase inhibitors for the treatment of rheumatoid arthritis demonstrate similar profiles of in vitro cytokine receptor inhibition. *Pharmacol Res Perspect* **7**:e00537.

Gooderham MJ, Forman SB, Bissonnette R, Beebe JS, Zhang W, Banfield C, Zhu L, Papacharalambous J, Vincent MS, and Peeva E (2019) Efficacy and safety of oral Janus kinase 1 inhibitor abrocitinib for participants with atopic dermatitis: A Phase 2 randomized clinical trial. *JAMA Dermatol* **155**:1371-1379.

Leclercq L, Cuyckens F, Mannens GSJ, de Vries R, Timmerman P, and Evans DC (2009) Which human metabolites have we MIST? Retrospective analysis, practical aspects, and perspectives for metabolite identification and quantification in pharmaceutical development. *Chem Res Toxicol* **22**:280-293.

Peeva E, Hodge MR, Kieras E, Vazquez ML, Goteti K, Tarabar SG, Alvey CW, and Banfield C (2018) Evaluation of a Janus kinase 1 inhibitor, PF-04965842, in healthy subjects: a phase

1, randomized, placebo-controlled, dose-escalation study. *Br J Clin Pharmacol* **84**:1776-1788.

Riccardi K, Lin J, Li Z, Niosi M, Ryu S, Hua W, Atkinson K, Kosa RE, Litchfield J, and Di L (2017) Novel method to predict in vivo liver-to-plasma K_{puu} for OATP substrates using suspension hepatocytes. *Drug Metab Dispos* **45**:576-580.

Silverberg JI, Simpson EL, Thyssen JP, Gooderham M, Chan G, Feeney C, Biswas P, Valdez H, DiBonaventura M, Nduaka C, and Rojo R (2020) Efficacy and safety of abrocitinib in subjects with moderate-to-severe atopic dermatitis: a randomized clinical trial. *JAMA Dermatol* **156**:863-873.

Simpson EL, Sinclair R, Forman S, Wollenberg A, Aschoff R, Cork M, Bieber T, Thyssen JP, Yosipovitch G, Flohr C, Magnolo N, Maari C, Feeney C, Biswas P, Tatulych S, Valdez H, and Rojo R (2020) Efficacy and safety of abrocitinib in adults and adolescents with moderate-to-severe atopic dermatitis (JADE MONO-1): a multicentre, double-blind, randomised, placebo-controlled, phase 3 trial. *Lancet* **396**:255-66.

Spracklin DK, Chen D, Bergman AJ, Callegari E, and Obach RS (2020) Mini-review: comprehensive drug disposition knowledge generated in the modern human radiolabeled ADME study. *CPT Pharmacometrics Syst Pharmacol* **9**:428-434.

Trier AM and Kim BS (2018) Cytokine modulation of atopic itch. *Curr Opin Immunol* **54**:7-12.

van Duijn E, Sandman H, Grossouw D, Mocking JA, Coulier L, and Vaes WHJ (2014) Automated combustion accelerator mass spectrometry for the analysis of biomedical samples in the low attomole range. *Anal Chem* **86**:7635-7641.

Walsky RL, and Obach RS (2007) A comparison of 2-phenyl-2-(1-piperidinyl)propane (PPP), 1,1′,1″-phosphinothioylidynetrisaziridine (ThioTEPA), clopidogrel, and ticlopidine as selective inactivators of human cytochrome P450 2B6. *Drug Metab Dispos* **35**: 2053–2059.

Wang EQ, Le V, Winton JA, Tripathy S, Raje S, Wang L, Dowty ME, and Malhotra BK (2021a) Effects of renal impairment on the pharmacokinetics of abrocitinib and its metabolites. *J Clin Pharmacol* doi: 10.1002/jcph.1980.

Wang EQ, Le V, O'Gorman M, Tripathy S, Dowty ME, Wang L, and Malhotra BK (2021b) Effects of hepatic impairment on the pharmacokinetics of abrocitinib and its metabolites. *J Clin Pharmacol* **61**:1311-1323.

Wang X, Dowty ME, Wouters A, Tatulych S, Connell CA, Le VH, Tripathy S, O'Gorman MT, Winton JA, Yin N, Valdez H, and Malhotra BK (2022) Assessment of the effects of inhibition or induction of CYP2C19 and CYP2C9 enzymes, or inhibition of OAT3, on the pharmacokinetics of abrocitinib and its metabolites in healthy individuals. *Eur J Drug Metab Pharmacokinet*, In press.

Yang X, Atkinson K, and Di L (2016) Novel cytochrome P450 reaction phenotyping for low-clearance compounds using the hepatocyte relay method. *Drug Metab Dispos* **44**:460–465.

Fig. legends

Fig. 1. Dose-normalized log mean (± standard deviation) plasma concentration-time profiles (linear inset) for abrocitinib (○ = 200 mg oral and ■ = 100 μg IV) and total radioactivity (Δ = 80 μg oral) following single dose administration. IV, intravenous.

Fig. 2. Cumulative mean (± standard deviation) recovery of administered radioactivity in urine (85.0% ± 6.0%) and feces (9.5% ± 0.5%) following a single oral dose of 200 mg ^{14}C-abrocitinib (n=6). Total recovery was 94.5% ± 5.9%.

Fig. 3. Representative HPLC radiochromatograms of plasma (A), urine (B), and feces (C) following a single 200 mg dose of ^{14}C-abrocitinib. HPLC, high performance liquid chromatography; M, metabolite.

Fig. 4. Proposed metabolic pathways of abrocitinib following oral administration. M, metabolite.

Fig. 5. Proposed mass balance model for abrocitinib following oral administration. CL_p, plasma clearance; CLr, renal clearance; F, bioavailability; $f_a f_g$, fraction absorbed × fraction surviving gut metabolism; f_m, fraction of metabolism; V_{ss}, steady state volume of distribution.

Table 1. Mean pharmacokinetic parameters for abrocitinib following IV and oral administration

Plasma Pharmacokinetics

Parameter	^{14}C-Abrocitinib,[a] IV	Abrocitinib, Oral
Period	B	B
Dose, mg	0.1	200
Body weight, kg (SD)	83.1 (13.7)	83.1 (13.7)
AUC_{inf}, ng* h/mL	1.56 (15)	1850 (35)
C_{max}, ng/mL		778 (45)
T_{max}, h (range)		0.50 (0.5-2.0)
$t_{1/2}$, h (SD)	1.45 (0.08)	1.52 (0.09)
CL, L/h	64.2 (14)	
V_{ss}, L	100 (19)	
% Bioavailability F[b] (90% CI)		59.8 (45.9-77.8)

Urine Pharmacokinetics

Parameter	Total ^{14}C PO	Total ^{14}C IV
Period	A	B
% of ^{14}C dose in urine	85.1 (7)	93.3 (1)
% $f_a f_g$[c]	91.3	

Plasma pharmacokinetics were assessed during Period B using noncompartmental analysis of concentration–time data. Geometric mean values (% coefficient of variation) except mean body weight and $t_{1/2}$ (± standard deviation) and median T_{max} (range).

[a]Period B dosing: abrocitinib, 200 mg, orally, followed by an intravenous dose of ^{14}C-abrocitinib (5 minutes infusion) at ≈1 hour after oral dose.

[b] %F = 100% x $[AUC_{po}/AUC_{iv}] \times [Dose_{iv}/Dose_{po}]$

^{c} %f_af_g = 100% x [Total $^{14}C_{po}$/Total $^{14}C_{iv}$]

( )%CV, percentage coefficient of variation; AUC_{inf}, area under the concentration-time curve from time 0 to infinity; CL, clearance; C_{max}, maximum concentration; F, bioavailability; f_af_g, fraction absorbed × fraction surviving gut metabolism; $t_{1/2}$, half-life, T_{max}, time to maximum plasma concentration; V_{ss}, steady state volume of distribution.

Table 2. Abrocitinib and metabolites in pooled plasma, urine, and feces samples following a

single oral dose of 200 mg ^{14}C-abrocitinib (period A, n = 6). Identified analytes ordered in

relationship to prevalence in plasma

Analyte	Plasma (% of total radioactivity)	Urine[b] (% of dose)	Feces[b] (% of dose)	Total Urine/Feces (% of dose)
Abrocitinib	25.8	0.6	0.3	0.9
M4	13.8	15.4	0.3	15.7
M2[a]	12.4	13.5	0.5	14.0
M1	11.3	16.2	1.7	17.9
M3[a]	4.8	4.5	0.3	4.8
M7	4.6	5.6	1.5	7.1
M6	3.4	12.2	0.8	13.0
372-1	2.5	0.7	0.2	0.9
358-1	2.0	1.1	0.1	1.2
356-1a	1.5	1.7	0.2	1.9
356-2	1.5	3.3	0.6	3.9
M8	1.4	1.3	nd	1.3
340-5	1.0	0.4	0.2	0.6
M5	0.4	0.3	nd	0.3

[a]M2 and M3 are stereoisomers.

[b]Only percentages of identified metabolites are reported.

M, metabolite; nd, not detected.

Table 3. Molecular ions and characteristic fragment ions of abrocitinib and metabolites detected

in plasma and excreta

ID	Standard ID	Retention Time (min)	[M+H]$^+$ m/z	Parent Fragments m/z	Diagnostic Fragments m/z
M6	PF-07095462	3.4	370.1179	70	217, 165
340-5		4.9	340.1074	201, 176, 175, 149, 70	296
372-1		5.0	372.1334	176, 70	
M7	PF-06737821	5.2	354.1230	201, 175, 149, 70	218
M8	PF-07055039	5.8	356.1387	70	217, 165
358-1		6.1	358.1543	176, 70	235, 217, 183, 165
356-1a		6.4	356.1386	70	217, 192, 191, 165
356-2		6.5	356.1384	176, 70	233, 207, 181
M1	PF-06471658	7.6	340.1438	201, 175, 149, 70	218
M2	PF-07055087	8.5^a	340.1438	201, 175, 149, 70	218
M3	PF-07055090	8.5^a	340.1438	201, 175, 149, 70	218
M4	PF-07054874	10.0^b	340.1438	176, 70	234, 217, 191, 165
M5	PF-07054926	10.0^b	310.1332	176, 70	204, 187, 161, 135
Abrocitinib	PF-04965842	11.5	324.1490	201, 176, 175, 149, 70	

[a]Co-eluting enantiomers followed by a second chromatographic separation (see Methods).

[b]Co-eluting peaks with subsequent identification from urine isolation and nuclear magnetic resonance

analyses (see Methods).

M, metabolite.

Table 4. Fractional clearance (f_{CL}) by metabolite determined from abrocitinib incubation in

human hepatocytes

Parameter	M1	M7	M2/M3	M4	358-1	372-1	149	Abrocitinib
% Radioactivity	5.6	0.35	4.2	3.6	0.16	0.16	0.42	85
Metabolite f_{CL}	0.39	0.024	0.29	0.25	0.011	0.011	0.029	-
Final f_{CL}	0.41		0.29		0.27		0.029	-

$f_{CL,}$ fractional clearance; M, metabolite.

Table 5. Enzyme kinetic parameters of abrocitinib metabolism in human liver microsomes using Michaelis-Menten substrate inhibition modeling

Kinetic Parameter	M1	M2/M3	M4	Total
K_m, μM	143 ± 20	251 ± 26	519 ± 100	-
V_{max}, pmol/min/mg	26.7 ± 2.2	73.8 ± 5.0	881 ± 125	-
K_i, μM	1480 ± 316	1680 ± 320	1340 ± 430	-
CL_{int}, μL/min/mg	0.187	0.294	1.7	2.18
$CL_{int,app,sc}$, mL/min/kg	0.176	0.278	1.6	2.05
Fractional Proportion $CL_{int,app,sc}$	0.086	0.136	0.780	

Data expressed as the mean +/- standard error of mean from triplicate replicates; unbound fraction ($f_{u,inc}$) of abrocitinib in human liver microsomes (0.3 mg/mL) was 1.

CL_{int}, intrinsic clearance; $CL_{int,app\ sc}$, scaled in vivo intrinsic clearance; $f_{u,inc}$, unbound fraction; K_i, inhibition constant for substrates exhibiting substrate inhibition kinetics; K_m, apparent substrate concentration at half-maximal velocity; M, metabolite; V_{max}, maximum rate of metabolism.

Table 6. Selective CYP chemical inhibition of abrocitinib metabolism in pooled human hepatocytes and overall fractional CYP pathway assignment (f_m)

Metabolite	f_{CL}	% CYP Inhibition (Scaled)				CYP Pathway f_m			
		2B6	2C9	2C19	3A4	2B6	2C9	2C19	3A4
M1 (M7)	0.41	16	24	52	8.0	0.066	0.10	0.22	0.033
M2/M3	0.29		44	55			0.13	0.16	
M4 (358-1, 372-1)	0.27		25	57	18		0.067	0.15	0.048
149	0.029				100				0.030
Overall f_m						0.066	0.30	0.53	0.11

Nonstatistical contributions by the remaining CYP isoforms for M1 (1A2, 2C8, 2D6), M2/M3 (1A2, 2B6, 2C8, 2D6, 3A), M4 (1A2, 2B6, 2C8, 2D6), and 149 (1A2, 2B6, 2C8, 2C9, 2C19, 2D6) were observed and excluded from fraction metabolized determinations. Fraction metabolized was calculated as the product of f_{CL} and fraction inhibited (scaled) as described in equation 7.

f_{CL}, fraction of clearance; f_m, fraction of metabolism; M, metabolite.

Table 7. In vitro enzymatic potency of abrocitinib and human metabolites M1, M2, and M4

JAK	IC_{50} (nM)[a]			
Assay	Abrocitinib	M1	M2	M4
JAK1	29.2	43.4	17.9	>10,000
JAK2	803	1140	886	>10,000
JAK3	>10,000	>10,000	>10,000	>10,000
TYK2	1250	3190	1210	>10,000

[a]IC_{50} values obtained at 1 mM adenosine triphosphate.

IC_{50}, half maximal inhibition concentration; JAK, Janus kinase; M, metabolite; TYK, tyrosine kinase.

Table 8. In vitro cellular potency of abrocitinib and human metabolites M1 and M2

Cytokine Induced pSTAT Assay				$IC_{50}/IC_{50,u}$ [a] (nM)		
Cytokine	JAK Pair	pSTAT	Cell Assay	Abrocitinib	M1	M2
IL-4	JAK1/JAK2	pSTAT6	Human keratinocytes	77.0	433	134
IL-13	JAK1/JAK2	pSTAT6	Human keratinocytes	81.9	236	84.1
IL-22	JAK1/TYK2	pSTAT3	Human keratinocytes	420	703	198
IL-31	JAK1/JAK2	pSTAT3	IFNγ primed THP-1	40.0	79.6	56.0
TSLP	JAK1/JAK2	pSTAT3	hWB (CD3$^+$ cells)	1020/343	785/438	271/152
IFNα	JAK1/TYK2	pSTAT3	hWB (lymphocytes)	174/58.5	296/165	90.5/50.6
IFNγ	JAK1/JAK2	pSTAT1	hWB (CD14$^+$ cells)	1690/569	1950/1090	2160/1210
IL-6	JAK1/JAK2	pSTAT1	hWB (CD3$^+$ cells)	343/115	171/95.3	136/76.0
IL-12	JAK2/TYK2	pSTAT4	hWB (lymphocytes)	9730/3270	33,400/18,600	5170/2890
IL-15	JAK1/JAK3	pSTAT5	hWB (lymphocytes)	537/181	558/311	353/197
IL-21	JAK1/JAK3	pSTAT3	hWB (lymphocytes)	516/174	844/471	487/272
IL-23	JAK2/TYK2	pSTAT3	hWB (lymphocytes)	>16,500/>5550	26,200/14,600	6210/3470
IL-27	JAK1/JAK2	pSTAT3	hWB (lymphocytes)	228/76.7	382/213	234/131
EPO	JAK2/JAK2	pSTAT5	hWB (spiked CD34$^+$ cells)	7180/2420	9750/5440	9470/5290

[a]hWB $IC_{50}/IC_{50,u}$: Total IC_{50}/Unbound IC_{50}; Unbound IC_{50} = hWB IC_{50} × (f_u/B/P ratio); Abrocitinib f_u =

0.36; M1 f_u = 0.63; M2 f_u = 0.71; abrocitinib B/P = 1.07; M1 B/P = 1.13; M2 B/P = 1.27; Mean IC_{50} from at

least two experiments.

B/P, blood/plasma ratio; EPO, erythropoietin; f_u, fraction plasma unbound; hWB, human whole blood; IC_{50},

half maximal inhibition concentration; IFN, interferon; IL, interleukin; JAK, Janus kinase; M, metabolite;

pSTAT, phospho-signal transducer and activator of transcription; TYK, tyrosine kinase; TSLP, thymic

stromal lymphopoietin.
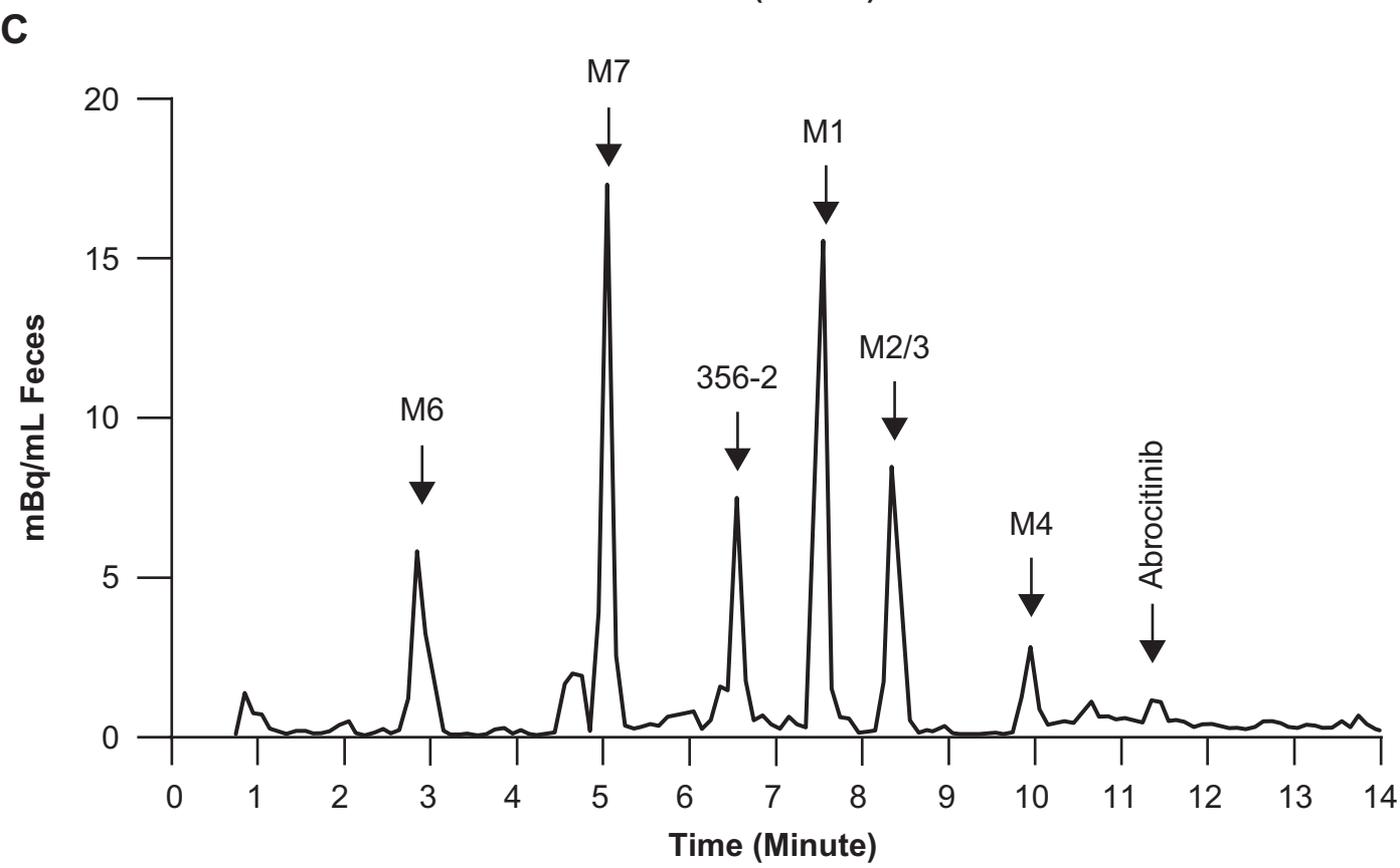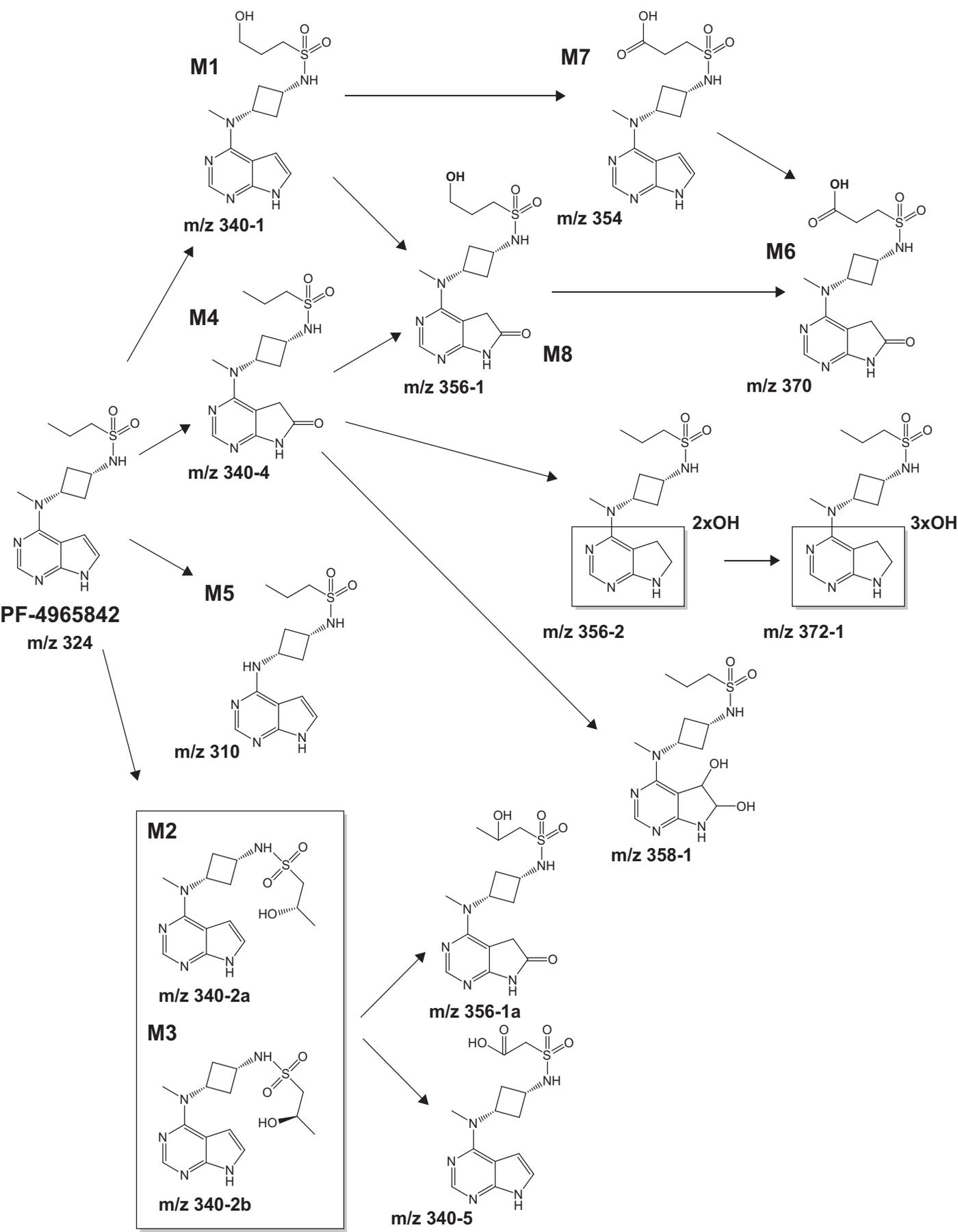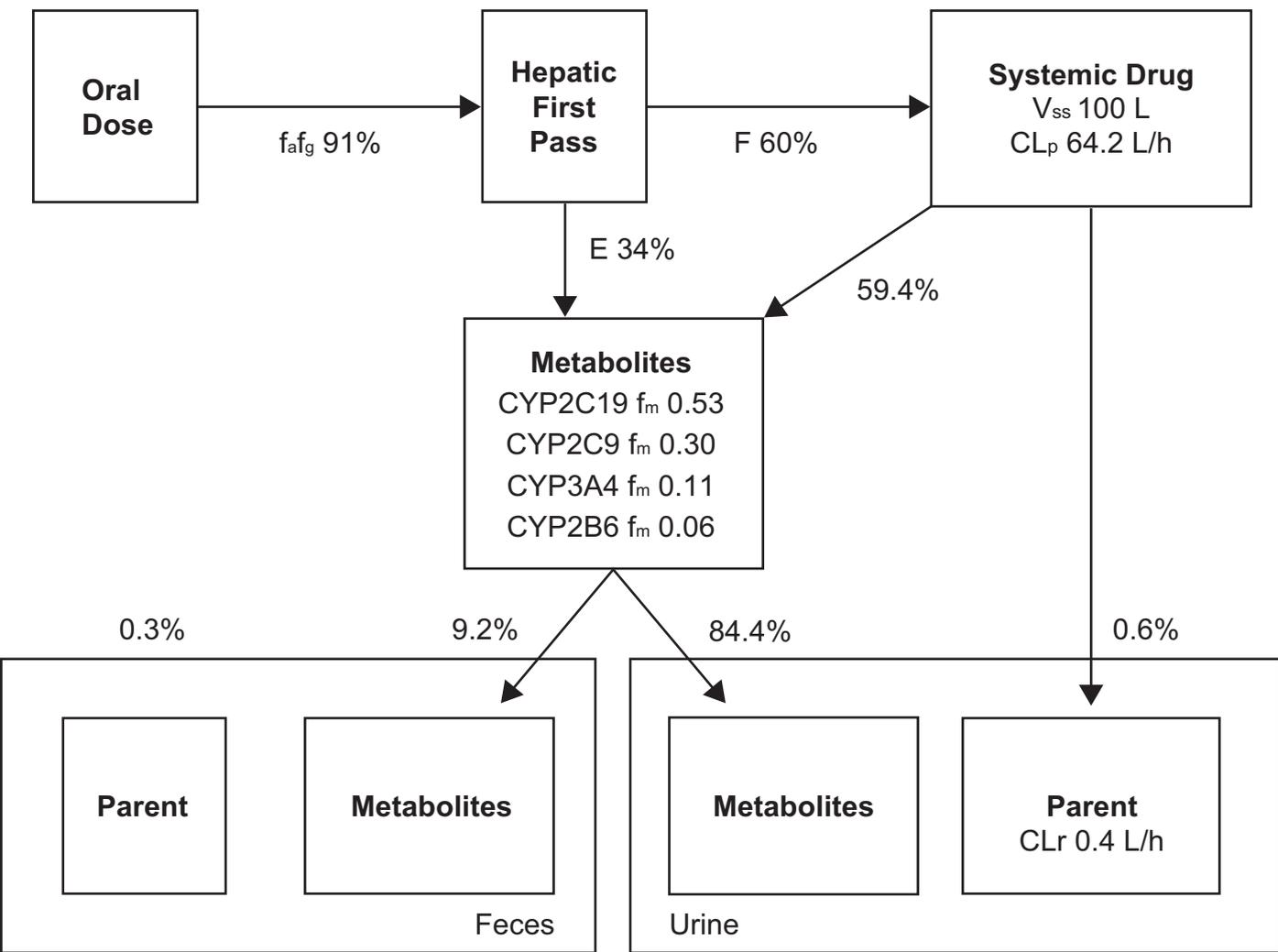
FIGURE 1
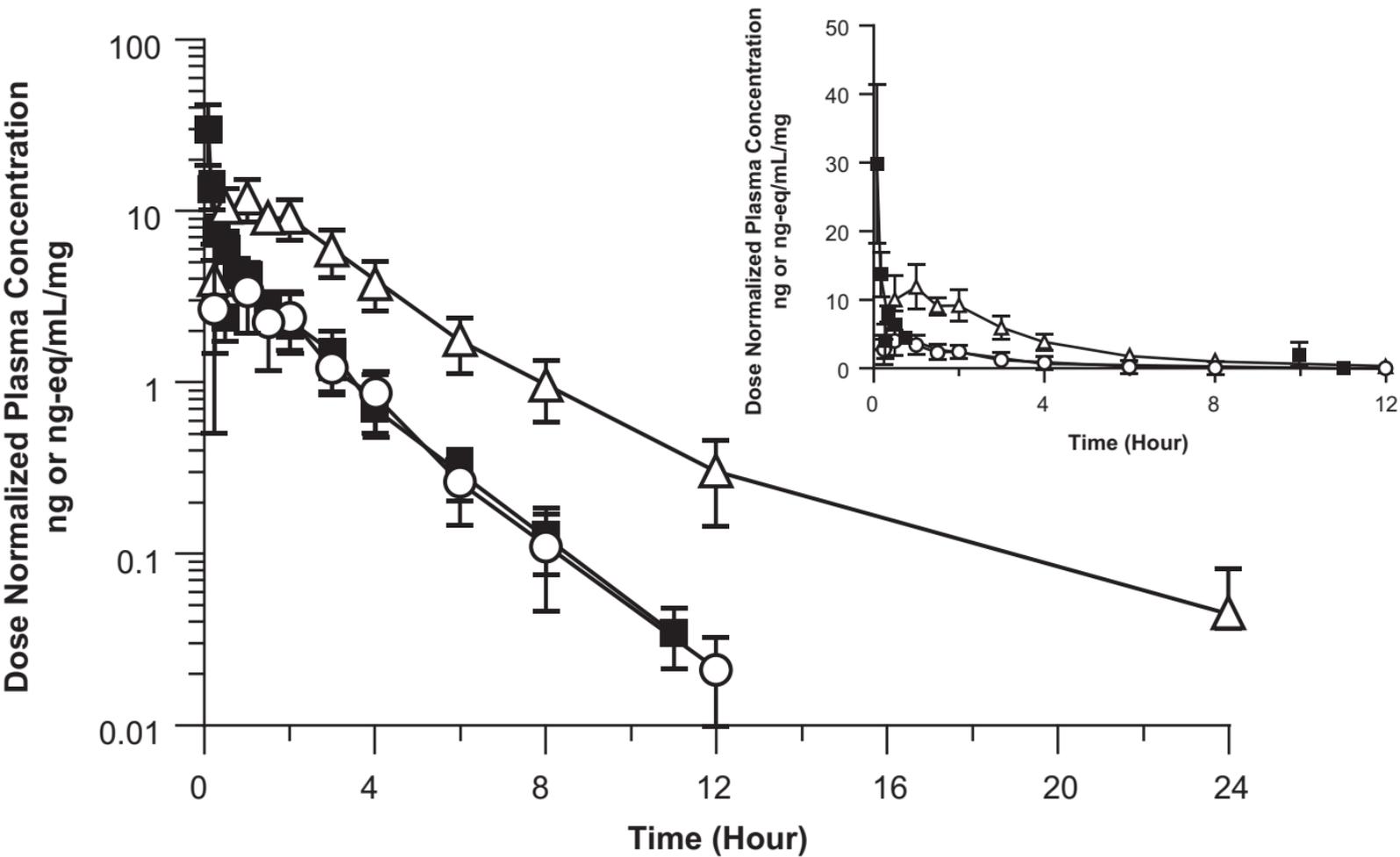
FIGURE 2
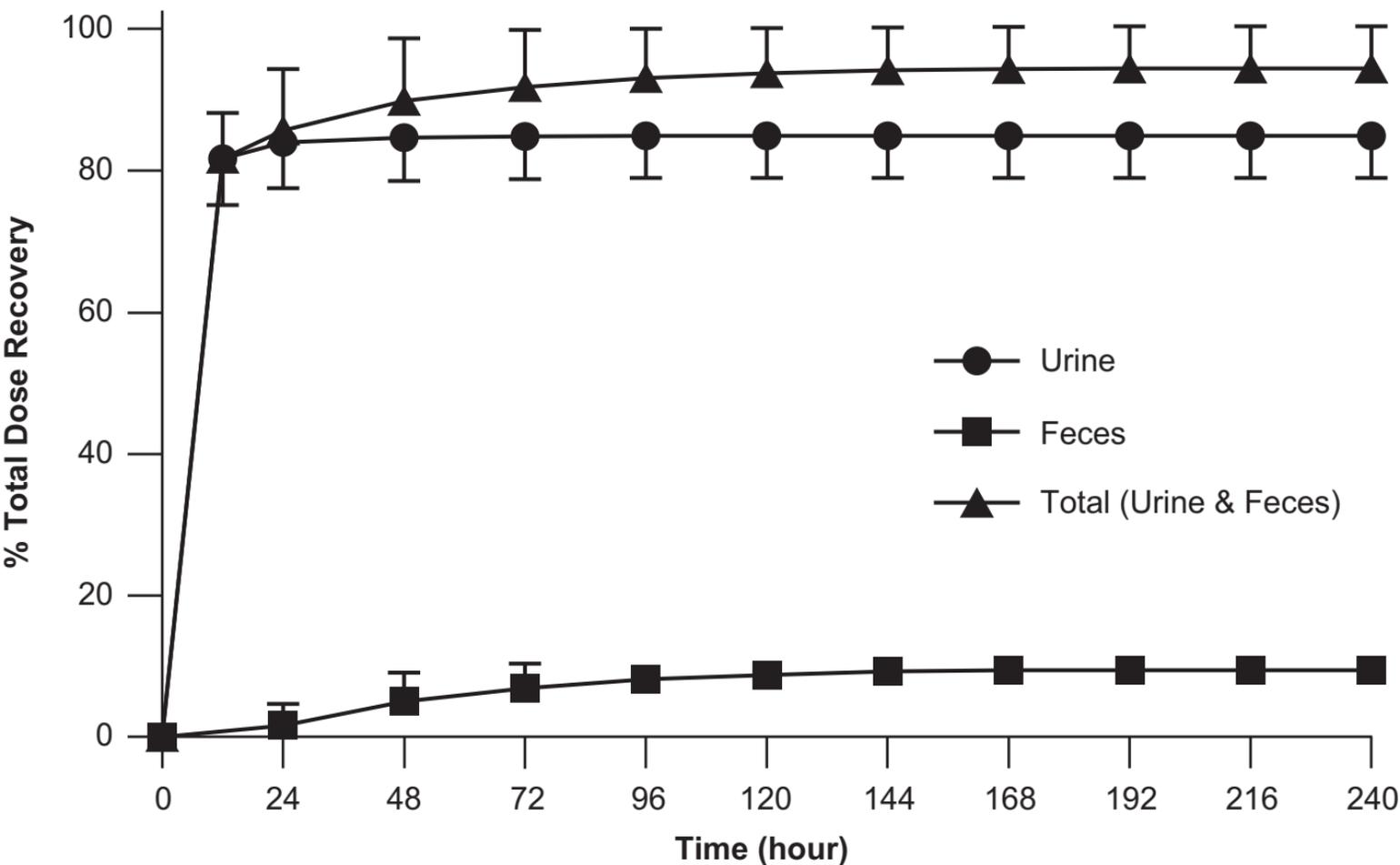
FIGURE 3

A
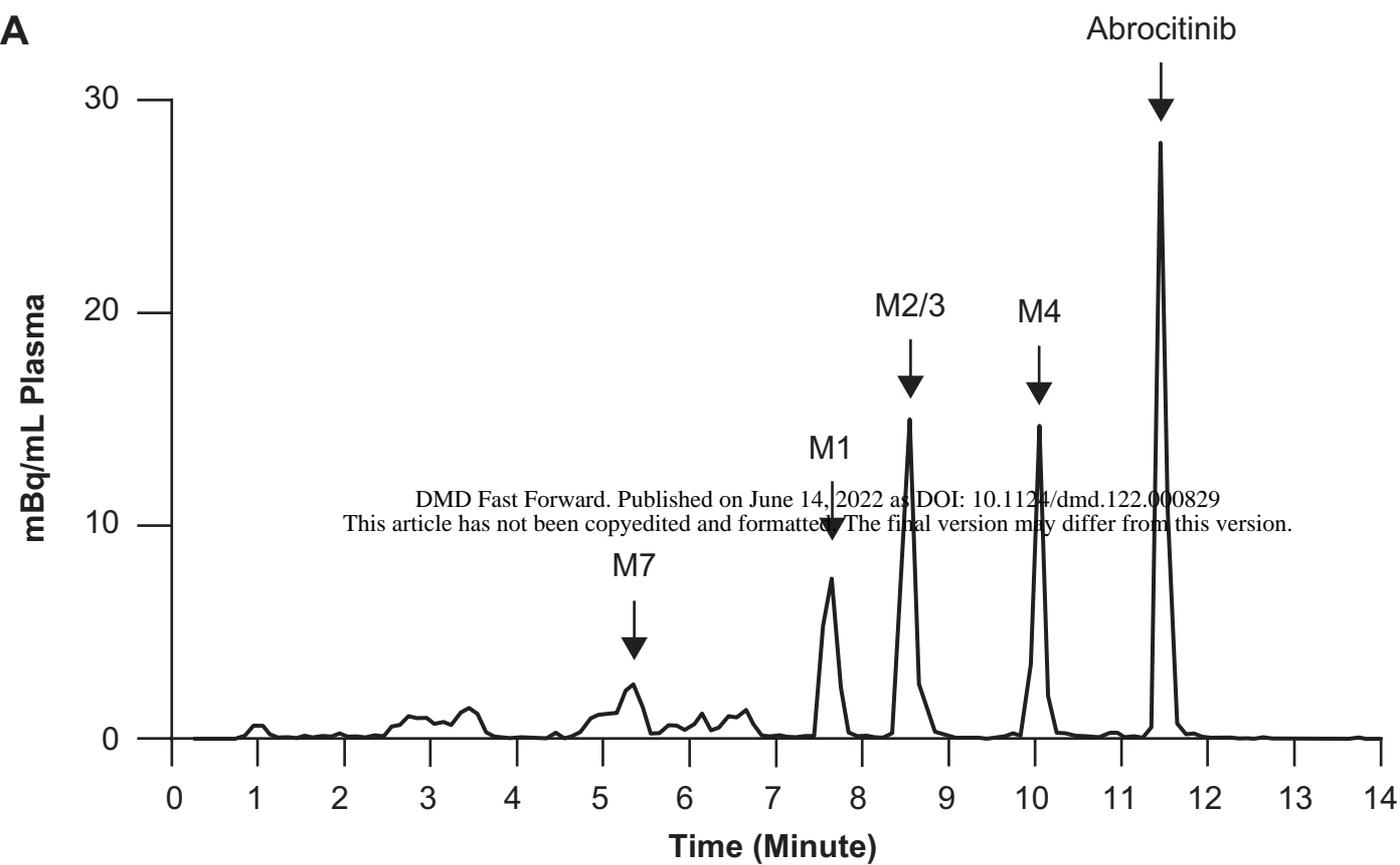
B
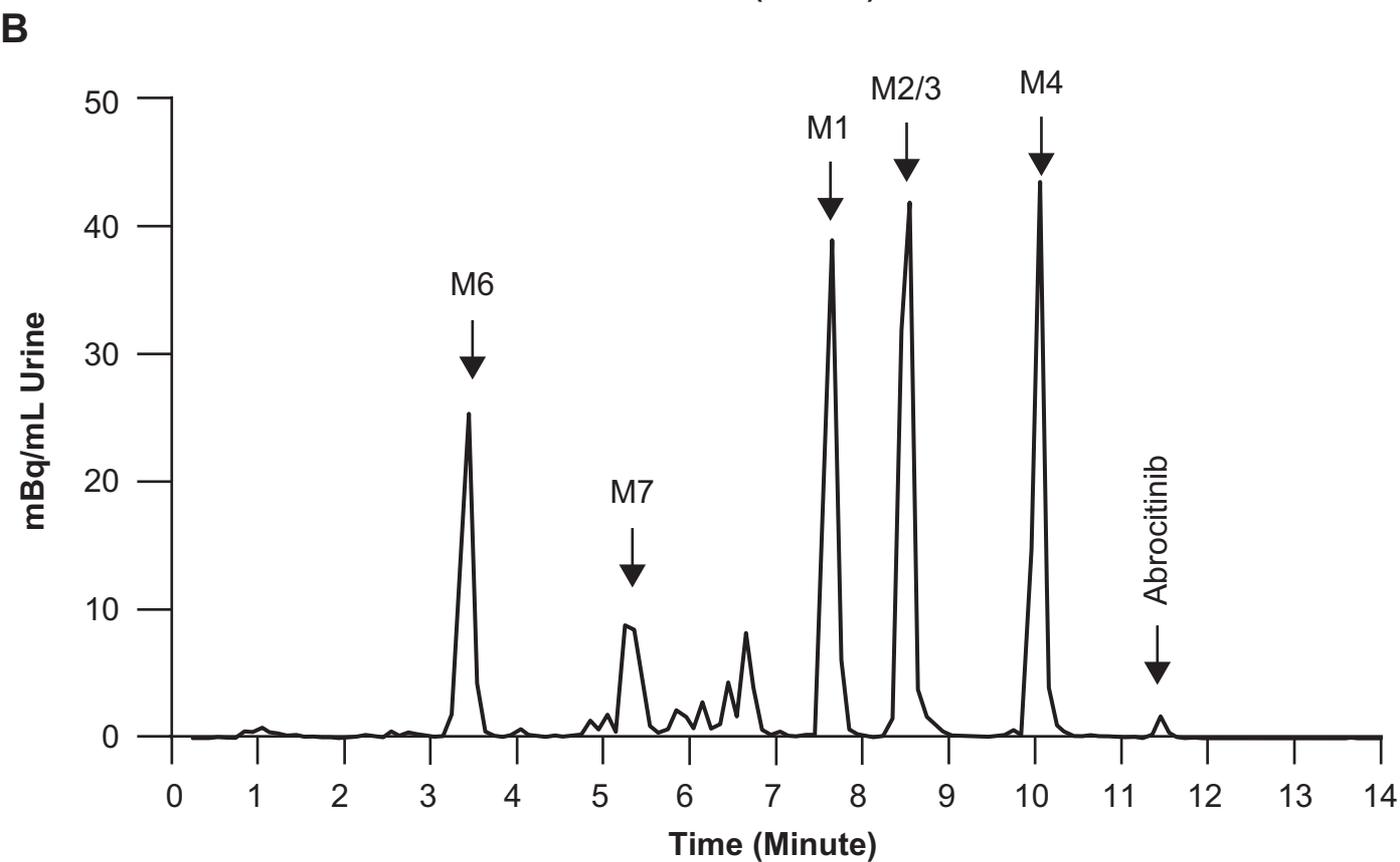
C

FIGURE 4

FIGURE 5

Total recovery 94.5%